AD-A156 944 VIBRO-ACOUSTIC FORECAST FOR SPACE SHUTTLE LAUNCHES AT VANDENBERG AFB: THE..(U) WESTON OBSERVATORY MA F A CROWLEY ET AL. 31 OCT 84 SCIENTIFIC-2 1/1

UNCLASSIFIED AFGL-TR-84-0322 F19628-84-C-0011 F/G 22/4 NL

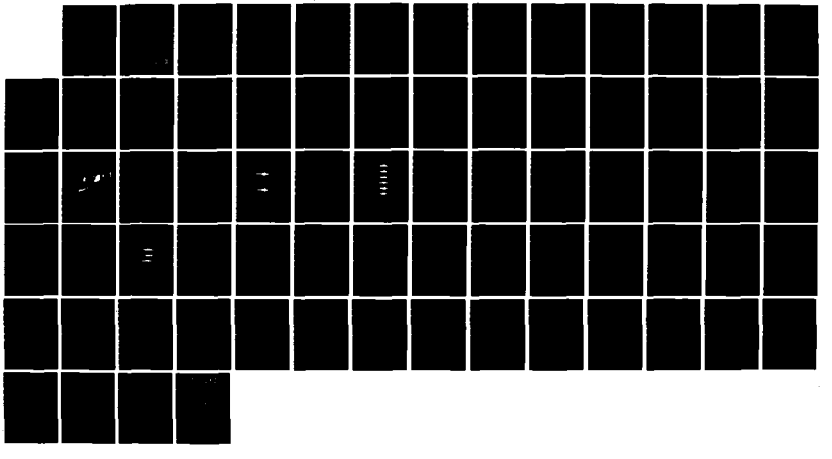

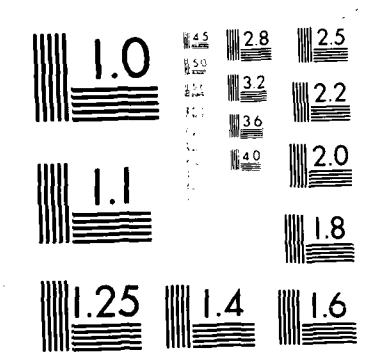

(2)

AFGL-TR-84-0322

# VIBRO-ACOUSTIC FORECAST FOR SPACE SHUTTLE LAUNCHES AT VANDENBERG AFB: THE PAYLOAD CHANGEOUT ROOM AND THE ADMINISTRATION BUILDING



Francis A. Crowley
Eugene B. Hartnett

Weston Observatory
Department of Geology and Geophysics
Boston College
381 Concord Road
Weston, Massachusetts 02193

31 October 1984

Scientific Report No. 2

Approved for Public Release; Distribution Unlimited



Air Force Geophysics Laboratory
Air Force Systems Command
United States Air Force
Hanscom AFB, Massachusetts 01731

CONTRACTOR REPORTS

This technical report has been reviewed and is approved for publication.

HENRY A. OSSING
Contract Manager

HENRY A. OSSING
Chief, Solid Earth Geophysics Branch

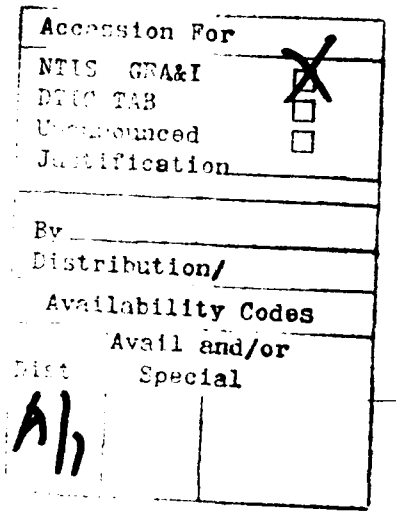


FOR THE COMMANDER

DONALD H. ECKHARDT
Director
Earth Sciences Division

This report has been reviewed by the ESD Public Affairs Office (PA) and is releasable to the National Technical Information Service (NTIS).

Qualified requestors may obtain additional copies from the Defense Technical Information Center. All others should apply to the National Technical Information Service.

If your address has changed, or if you wish to be removed from the mailing list, or if the addressee is no longer employed by your organization, please notify AFGL/DAA, Hanscom AFB, MA 01731. This will assist us in maintaining a current mailing list.

UNCLASSIFIED

SECURITY CLASSIFICATION OF THIS PAGE

AD-A156944

# REPORT DOCUMENTATION PAGE

| | |
|---|---|
| 1a. REPORT SECURITY CLASSIFICATION: UNCLASSIFIED | 1b. RESTRICTIVE MARKINGS |
| 2a. SECURITY CLASSIFICATION AUTHORITY | 3. DISTRIBUTION/AVAILABILITY OF REPORT: APPROVED FOR PUBLIC RELEASE; DISTRIBUTION UNLIMITED |
| 2b. DECLASSIFICATION/DOWNGRADING SCHEDULE | |
| 4. PERFORMING ORGANIZATION REPORT NUMBER(S) | 5. MONITORING ORGANIZATION REPORT NUMBER(S): AFGL-TR-84-0322 |
| 6a. NAME OF PERFORMING ORGANIZATION: Weston Observatory, Boston College / 6b. OFFICE SYMBOL (If applicable) | 7a. NAME OF MONITORING ORGANIZATION: Air Force Geophysics Laboratory, Earth Sciences Division |
| 6c. ADDRESS (City, State and ZIP Code): 381 Concord Road, Weston, MA 02193 | 7b. ADDRESS (City, State and ZIP Code): Hanscom AFB, MA 01731; Contract Manager: Henry A. Ossing |
| 8a. NAME OF FUNDING/SPONSORING ORGANIZATION: Same as Block 7a / 8b. OFFICE SYMBOL (If applicable) | 9. PROCUREMENT INSTRUMENT IDENTIFICATION NUMBER: F19628-84-C-0011 |
| 8c. ADDRESS (City, State and ZIP Code) | 10. SOURCE OF FUNDING NOS |

| PROGRAM ELEMENT NO | PROJECT NO | TASK NO | WORK UNIT NO |
|---|---|---|---|
| 62101F | 7600 | 09 | AF |

11. TITLE (Include Security Classification): * See Block No 16

12. PERSONAL AUTHOR(S): CROWLEY, Francis A.; HARTNETT, Eugene B.

| 13a. TYPE OF REPORT | 13b. TIME COVERED | 14. DATE OF REPORT (Yr., Mo., Day) | 15. PAGE COUNT |
|---|---|---|---|
| Scientific Rpt No 2 | FROM ____ TO ____ | 84/10/31 | 71 |

16. SUPPLEMENTARY NOTATION: * Block 11 * Vibro-Acoustic Forecast for Space Shuttle Launches at Vandenberg AFB: The Payload Changeout Room and the Administration Building

| 17. COSATI CODES | | |
|---|---|---|
| FIELD | GROUP | SUB GR |
| 08 | 11 | |
| 20 | 01 | |

18. SUBJECT TERMS (Continue on reverse if necessary and identify by block number): *Rocket Plume Acoustics; STS Launch Environment; Vandenberg AFB; Vibro Acoustics

19. ABSTRACT (Continue on reverse if necessary and identify by block number)

The PCR and AB vibro-acoustic environment is simulated for Shuttle launches at Vandenberg AFB using local responses and a source term founded on KSC launch pressures. Overpressure emanating from above the Launch Mount at VAFB is materially altered in form and level by site reverberations. Motion produced in simulations regularly approaches or exceeds velocity and acceleration thresholds cited for other launch support structures. Forecasts call for PCR roof displacements toward the PPR exceeding 2.0 cm for most launches. The expected maximum displacement after 5 launches is 3.5 cm. An exceedance of 5 cm can be anticipated over the facility life cycle (≈ 100 launches).

| 20. DISTRIBUTION/AVAILABILITY OF ABSTRACT | 21. ABSTRACT SECURITY CLASSIFICATION |
|---|---|
| UNCLASSIFIED/UNLIMITED ☒ SAME AS RPT ☐ DTIC USERS ☐ | UNCLASSIFIED |

| 22a. NAME OF RESPONSIBLE INDIVIDUAL | 22b. TELEPHONE NUMBER (Include Area Code) | 22c. OFFICE SYMBOL |
|---|---|---|
| Henry A. Ossing, AFGL/LWH | 617-861-3222 | LWH |

DD FORM 1473, 83 APR EDITION OF 1 JAN 73 IS OBSOLETE

UNCLASSIFIED

TABLE OF CONTENTS


| | | PAGE |
|---|---|---|
| 1.0 | INTRODUCTION | 1 |
| 1.1 | Statement of Need | 1 |
| 1.2 | Scope | 1 |
| 1.3 | Approach | 1 |
| 2.0 | GSS LAUNCH ENVIRONMENT SPECIFICATIONS | 2 |
| 2.1 | Definitions | 2 |
| 2.1.1 | Motion Estimates | 2 |
| 2.1.2 | Pressure Estimates | 2 |
| 2.2 | Launch Environment Specifications | 3 |
| 2.2.1 | Motion | 3 |
| 2.2.2 | Pressure | 3 |
| 3.0 | FINDINGS | 4 |
| 3.1 | Motion | 4 |
| 3.2 | Pressure | 4 |
| 4.0 | PRESSURE FORECASTS | 5 |
| 4.1 | Introduction | 5 |
| 4.2 | Pressure Representations | 6 |
| 4.2.1 | Shuttle Source | 6 |
| 4.2.2 | Explosion Source | 7 |
| 4.3 | Source Mapping Operator | 7 |

PAGE

4.4 Simulation Source Error 8

4.5 Launch Pressure Simulations 9

4.5.1 East Face of PPR 9

4.5.2 AB Roof 10

5.0 MOTION FORECASTS 11

5.1 Motion Representation 11

5.2 Responses 12

5.3 PCR Motion Simulations 12

5.3.1 Particle Velocity 12

5.3.2 Displacement 13

5.3.3 Acceleration 13

5.3.4 Pseudo Velocity Estimates 13

5.4 Administration Building Motion 14

5.5 Repeated Launches 15

5.6 Summary 17

Figures 21

Appendix A: The Sounding Program 44

Table 1A: Sounding Tests 46

Figure 1A: Channel Responses 47

Figure 2A: Channel Responses 48

Figure 3A: Wavelets; 2.5 Pound Shot 49

Figure 4A: Wavelets; 2.5 Pound Shot 50

PAGE


Appendix B: Flat-Earth Vibro-Acoustics 51

Figure 1B: Vibro-Acoustic Shot Wavelets 53

Figure 2B: Sensor Configuration 54

Figure 3B: Channel Responses (1-6) 55

Figure 4B: Channel Responses (7-12) 56

Figure 5B: Channel Responses (13-18) 57

Figure 6B: Phase Velocity 58

Appendix C: Pseudo Velocity Spectra 59

References 60

Acronyms and Abreviations 64

## 1.0 INTRODUCTION

1.1 Statement of Need - There is a need to forecast the vibro-acoustic environment produced by Space Transportation System (STS) launches at Vandenberg Air Force Base (VAFB) to support facility design, operations and lifetime predictions.

1.2 Scope - Figure 1 shows the major Ground Support System (GSS) elements neighboring the launch pad. Our report treats launch vibro-acoustics for two of these structures: the Payload Changeout Room (PCR) and the Administration Building (AB). The PCR is a multistoried mobile structure used to carry payloads from the Payload Preparation Room (PPR) to the Shuttle on the Launch Mount (LM). The AB is the fixed building in the foreground of Figure 1, south of the PPR.

Prior to launch, the PCR is rolled back from the LM and parked just off the east face of the PPR. At launch time the PCR, PPR and AB are three distinct, tightly clustered multistoried structures. For small motions, the buildings move freely of one another. For displacements in excess of a few centimeters, they will collide. Secondary motion produced by pounding is outside the scope of this study; only the likelihood of impact is considered.

1.3 Approach - Vibro-acoustic forecasts presented here combine a Shuttle source term established at Kennedy Space Center (KSC) (1,2) with measured responses to small test explosions taken at VAFB, Appendix A. These responses contain site peculiar reverberations to be encountered during a STS launch at VAFB. Effects due to the rocket exhaust cloud and incomplete construction are not included in these estimates. It is believed their omission will not materially degrade the forecasts.

## 2.0 GSS LAUNCH ENVIRONMENT SPECIFICATIONS

2.1 Definitions - Motion environment can be specified in many ways (3). Peak motion is commonly cited, as is level. Both peak and level thresholds have the advantage that they are readily validated with minimal analysis and interpretation. For major structural members, more comprehensive measures such as pseudo response spectra or power spectra are usually invoked. In order to satisfy a variety of often cited motion specifications, we quantify Shuttle launch vibro-acoustics in the band 0.3 to 30 Hz as follows:

2.1.1 Motion Estimates

a) Peak Motion: The maximum component motion of a point from its long-term rest value.

b) Response Spectra: The maximum motion over a family of second order systems having 2% or 5% damping excited by a prescribed base motion.

c) Motion level: The root mean square motion of a point about its rest value over a duration T, starting at time t.

d) Power Spectra: Periodogram average based on motion samples of duration T.

2.1.2 Pressure Estimates

Pressure descriptors also have several variants. Pressure forecasts are given in terms of the following:

a) Peak Pressure: The largest observed pressure deviation from ambient.

b) Third-octave level: The root mean square pressure in third octave bands centered at frequencies, $f_c$, over a duration T, starting at time t.

c) Power Spectra: Periodogram average of pressure samples of

duration T.

d) OASPL: Broadband mean square pressure estimate determined by integrating the "best fitting" standard form spectra.

2.2 Launch Environment Specifications

2.2.1 Motion - Motion specifications have not been established for either the PCR or AB. However, acceleration spectra in excess of $.01g^2/Hz$ and pseudo velocity responses in excess of 100 inches/second are cited as motions of concern for other GSS structures (3). To these "thresholds of concern" we add a peak displacement that is half the prelaunch at-rest gap with the PFR. For the PCR, a west displacement as small as 1.0 centimeter can be a motion of concern, while a north displacement of 2.6 centimeters constitutes a "motion of concern" for the AB (4).

2.2.2 Pressure - Far-field acoustic estimates for launches at Station V23 have not seriously treated pressure modifications caused by topography and GSS structures (5). The forecasted OASPL maximum from 6.4% model studies coincides with our findings for a flat open area.

## 3.0 FINDINGS

Launch motion forecasts are summarized in Table 1 for points on the south Payload Ground Handling Mechanism (PGHM) rails and the Orbiter Flight Simulator (OFS) floor. The locations were selected by the Shuttle Activation Task Force (SATAF). The table elements give the maximum value obtained in one simulated launch. Motion values approaching or exceeding thresholds of concern are highlighted.

3.1 Motion - Launch generated side-on pressure on the east face of the PCR will torque the structure into a lightly damped sway in line with the Launch Mount and the PPR. The motion forecast for the PCR regularly exceeds the displacement threshold of concern. A 5.0 cm prelaunch "at rest" gap between the PCR and the PPR is insufficient to regularly accommodate the expected sway of both buildings. The structures ran a high risk of pounding during a launch. The rebounding characteristics and subsequent damage from such collisions are outside the scope of the present study.

3.2 Pressure - The protusion of multistoried structures in the immediate neighborhood of the Launch Mount produces reverberations that significantly alter the phase, level and spectral characteristics of load acoustics impinging on the PCR and PPR. Forecasts that include site reverberations obtained in sounding tests call for pressure spectra on the east face of PPR at each is 10 db higher than spectra at a flat-earth site for the same distance.

OASPL contour maps for the launches at uncluttered flat-earth sites like [illegible] are useful because such places do not materially reshape load spectra. In contrast, OASPL contour maps for VAFB are of limited utility because reverberations alter the spectral content and phasing of the applied loads on structures neighboring the Launch Mount.

## 4.0 PRESSURE FORECASTS

4.1 Introduction - Pressures outside a source region can be separated into a free-field term and contributions arising from boundaries. For a small source in an isothermal, windless atmosphere overlying a dense, flat, perfectly reflecting earth, the surface boundary doubles the incident free-field pressure term (6). For a less than perfectly reflecting flat-earth, surface pressure depends on the path defined by the source and measurement locations.

Surface pressure produced by a Shuttle launch at KSC is well represented by small source, far-field, spherical acoustics incident on a flat-earth for stations clear of the rocket exhaust groundcloud. Surface pressures at offsets in the range of 200 to 400 meters decay inversely with range without a change in form, with phase delays in harmony with the pressure field produced by a point source imbedded in the rocket plume moving with the Shuttle (1,2). Around the time of maximum loading, STS launch overpressures satisfy standard form undeflected plume spectra (2).

The OASPL maximum at KSC for 2.56 second averaging at stations 300 meters from the launch pad, clear of the groundcloud, occurs about 11 seconds after liftoff with the Shuttle at an altitude of 300 meters. At this time the equivalent acoustic source is 100 meters below the Shuttle (2). The OASPL maximum is 148 db (151 db for 0.3 second averaging) (2). The spectral maximum is around 7.0 Hz, a value in harmony with scaling estimates that use the propulsion system parameters (7,8).

4.2 Pressure Representations:

4.2.1 Shuttle Source - Launch generated surface overpressure time histories around the OASPL maximum at an offset of 300 meters are simulated by convolving an independent, zero mean, unit variance, normal process, N(0,1) with a STS source term, $Y_{STS}(t)$ and a site response $\phi(a_s,h;t)$.

$$P_{STS}(a_s;t) = \phi(a_s,h;t) * Y_{STS}(t) * N(0,1)$$

$$(a_s^2 + h^2)^{1/2} \approx 350 \text{ meters}$$

In this construction, $\phi$ connects the pressure developed at the ground surface to a source pressure emitted by the propulsion system. It includes all contributions caused by site boundaries while the shaping term, Y, is solely a source attribute of the incident free-field pressure, independent of boundary contributions.

Shortly before and following the OASPL maximum, spectral shape at points neighboring the Shuttle launch is relatively constant. The conspicuous change for a fixed observer monitoring a moving rocket is in sound power level. The nonstationary characteristic in acoustic level for a launch is incorporated into our simulation by an empirical envelope function, $E(a_s,t)$ giving:

$$P_{STS}(a_s,t) = \phi_{ff}(a_s,h;t) * [\quad] * [\quad] * N(0,1) * \frac{e^{ik(r-a_s)}}{a_s + (a_s/2)^2 (r-a_s)}$$

TABLE 2

V23 ACOUSTIC ENVIRONMENT (db)

THIRD OCTAVE

| HZ | PPR (East Wall) | AB (Reef) | 6.47 | Flat-Earth Area | Observed KE 261 meters STS 11 |
|---|---|---|---|---|---|
| 4.0 | 142.2 | 139.1 | - | 139.8 | 135.6 |
| 5.0 | 148.2 | 143.8 | - | 136.7 | 139.0 |
| 6.3 | 142.9 | 137.9 | | 137.2 | 139.5 |
| 8.0 | 140.8 | 137.3 | - | 136.4 | 136.5 |
| 10.0 | 141.7 | 138.7 | - | 137.5 | 137.2 |
| 12.5 | 146.4 | 140.7 | - | 136.9 | 140.4 |
| 16.0 | 146.4 | 141.2 | 129.5 | 137.1 | 136.8 |
| 20.0 | 145.8 | 140.8 | 131.0 | 136.7 | 138.3 |
| 25.0 | 145.5 | 138.7 | 133.0 | 134.8 | 139.5 |
| OASPL | 155.7 | 150.5 | 14[illegible] | 148.3 | 148.5 |

TABLE 1

PEAK MOTION VALUES

BANDPASS $0.3 < f < 30$ Hz; Launch #6; A3

| LOCATION | DISPLACEMENT (cm) | VELOCITY (cm/sec) | ACCELERATION (g) |
|---|---|---|---|
| PCR: | | | |
| UPPER SOUTH PGHM RAIL | | | |
| Z | 0.43 | 3.4 | .15 |
| N | 0.46 | 4.7 | .16 |
| E | 2.32 | 21.6 | .34 |
| PCR: | | | |
| LOWER SOUTH PGHM RAIL | | | |
| Z | 0.74 | 6.6 | .55 |
| N | 0.21 | 2.5 | .09 |
| E | 0.52 | 6.5 | .24 |
| AE: | | | |
| OFS FLOOR | | | |
| Z | 0.41 | 9.3 | .73 |
| N | 0.26 | 2.9 | .11 |
| E | 0.37 | 3.7 | .14 |

be maintained between buildings, pounding is unlikely and our simulations should almost always apply. If the 10 cm gap cannot be maintained, pounding can again be avoided by hard coupling the structures to force them to move as a single system.

the PCR will exceed some threshold displacement, d, after a specific number of launches, N. The cumulative probability that the threshold, d, will be met or exceeded by the Nth launch is given by:

$$W(N) = 1-P(d)^N$$

From Figure 20, P=50% for steady state segments of slightly more than 2.0 seconds. The chance that 2.00 cm will be exceeded after 3 launches is 7 chances out of 8. Similiarly, there is a 50/50 chance that the PCR will exceed a displacement of 3.5 cm after 5 launches.

In the same way we generate the distribution for the vertical acceleration maxima from steady state samples, Figure 22. Using P(35)=50%, the OFS floor is expected to experience a peak acceleration of at least 0.7 g for most launches. Over a sequence of 5 launches there is a 50/50 chance that the OFS floor accelertation will exceed 0.85 g's.

5.6 Summary - Table 1 is a summary of peak launch motion values obtained by simulation. Motion maxima are given in terms of displacement, velocity and acceleration. The motions of concern are the east displacement of the upper PGHM rail and the vertical acceleration of the OFS floor. The peak motion over a sequence of launches varies by about a factor of 2. The distribution in the peak value is in harmony with the forecast obtained by segmenting a stationary process.

The at-rest gap between the PCR and PFR over a set of launches is itself an uncertain quantity subject to statistical description. The minimum gap between the hard roof edges measured August 1984 was something less than 1.0 cm. At that time, the PCR was skewed well out of alignment with the PFR. If a prelaunch at-rest gap as large as 10 cm can always

distribution is graphed in a manner that plots a Normal distribution as a straight line. The PCR displacement maxima are not distributed as a normal variate. They lie much closer to a Rayleigh population, the limiting distribution for maxima of a narrowband process. The figure gives the probability of containing the maximum displacement by the threshold based on assumptions about how long the PCR motion "essentially" holds a steady state characteristic during a launch; i.e., the average number of maxima encountered in the interval for $E(a_s; t) \approx 1$. The longer the motion persists, the larger the absolute maximum.

If we now treat each launch to be an independent event governed by the probability distribution P(d) shown in Figure 20, the maximum displacement of the PCR after a number of launches can be immediately forecast through the return period (18) defined by:

$$T(d) = \frac{1}{1-P(d)}$$

The expression is simply a statement that if the PCR has a single launch probability, $p = (1-P(d))$ of exceeding a threshold displacement, d, we must have, on the average, 1/p launches to exceed the threshold once.

Figure 21 is the maximum displacement forecast for the PCR roof based on the return period of steady state motion sample segments of between 2.00 and 3.00 second duration. The forecasted peak displacement is relatively insensitive to assumptions about envelope shape after a modest number of launches. Over a facility life cycle of 100 launches, the absolute maximum west displacement of the PCR from its prelaunch rest value is estimated to be 5 cm.

Viewed somewhat differently, we can estimate the probability that

histories exceed the cited $.01g^2/Hz$ threshold for a number of frequency bands, Figure 17. In contrast, pseudo velocity spectra are well below the 100 in/sec level, Figure 18. Even over a large sequence of launches, it is highly unlikely that OFS floor motion will exceed displacement or velocity thresholds of concern.

5.5 Repeated Launches - The maximum probable motion excited over a series of launches depends on structure response and the ensemble characteristics of the Shuttle source pressure being ultimately representable by a N(0,1) process.

The maximum motion forecast for a sequence of launches is based on the distribution of a stationary process, u (r,t) obtained by setting $E(r_s;t)=1$, leaving:

$$u_{S:S}(r;t) = u_{exp}(r;t) * W(t) * N(0,1)$$

where, as before, the motion produced by an explosion is represented by:

$$u_{exp}(r;t) = G(r;t) * Y_{exp}(t) * S(t)$$

for the path established by r.

Figure 19 is the distribution obtained for east displacement maxima of the upper PGHM rail when the PCR is excited, long term, with load values appropriate for around the time of the OASPL maximum. The maxima for such a construction are known to lie between a Rayleigh and Normal distribution, depending on spectral composition (17).

Figure 20 is the distribution in the absolute maxima of PCR root displacements in the direction of the PPR for different length samples based on the stationary process for the PGHM rail that preserves tilt. The

members like the PGHM rails can be treated as the input motion to attached components. Concern about the maximum motion excited in hardware during a launch naturally leads to the consideration of pseudo response spectra. For such analysis, a motion in excess of 100 in/sec has been cited as a "value of concern" in other GSS structures (3).

Figure 15 depicts pseudo velocity response spectra for 2% and 5% damping based on the upper and lower rail simulated motion, Appendix C. The results are plotted in a fashion that readily allows alternate estimates in terms of acceleration or displacement. The only motion approaching the 100 in/sec level is the east velocity of the upper PGHM rail. It can be expected that pseudo velocities for points above the upper PGHM rails will exceed 100 in/sec (254 cm/sec).

5.4 Administration Building Motion - In much the same manner as for the PCR, we construct launch generated time histories for the OFS floor in the Administration Building. Figure 16 shows floor accelerations based on response measurements constrained to a source height of less than 60 meters above the launch mount. Peak vertical acceleration in this case approaches 1.0 g. Since the simulation almost certainly underestimates roof loads generated by the Shuttle moving south and higher than 150 meters, true peak floor accelerations might well exceed 1.0 g.

Peak displacements of the AB normal to the gap with the FPR are substantially smaller than the at-rest opening. A design gap in excess of 5.0 cm should accommodate Administration Building displacements. Facility damage due to displacement should be confined to weak AB-FPR connecting elements.

OFS floor acceleration spectra based on 7.56 second time

PCR develops a secondary sway at right angles to the first but at a slightly higher frequency. This secondary sway is aggravated by the torque produced by reflections off the PPR that travel back along its south face. The horizonal motion is considerably larger at the upper elevation; the vertical motion is more intense near the base.

5.3.2 Displacement - Figure 12 recasts the motion given in Figure 11 into a displacement time history. As a result of sway, the upper rail executes an east displacement that is in phase, but larger in magnitude than that of the lower rail. The maximum tilt between the rails is $1*10^{-3}$ radians. A peak displacement at the roofline that preserves tilt implies a displacement 40% larger than shown for the upper PCHM rail. Displacements in the direction of the PPR should regularly exceed 2.0 cm. An at-rest gap of 5.0 cm or less between the two buildings is probably inadequate to avoid pounding. Our simulation, being based on a linear response, becomes invalid when pounding occurs. Pounding can be expected to substantially intensify motion in the PPR and PCR.

5.3.3 Acceleration - Figure 13 recasts the velocities given in Figure 11 into acceleration time histories. Lower rail acceleration spectra based on 2.56 second samples approach .01$g^2$/Hz, a threshold of concern for other facilities (3), Figure 14. True motion, unlike the simulated motion time histories, includes contributions above 30 Hz. Hence, actual peak acceleration should be somewhat larger than its corresponding simulated value. It is worth noting that acceleration spectra in this simulation are almost 3 orders of magnitude larger than observed for KSC ground stations at the same distance as the PCR (13).

5.3.4 Pseudo Velocity Estimates - Motion excited in major structura

a vertical trajectory, h=h(t):

$$u_k(PCR,t) = G(PCR,t;h,0) * p_{STS}(t)$$

As before, $p_{STS}$ (h,t) relates to $p_{exp}$ (h,t) through the mapping operator, W(t). G is determined by measurement over the path defined by its end points, namely the position of the "equivalent" STS source and location of the seismic observation.

5.2 Responses - G values from test shots are available for $15 < h < 60$ meters. In this range, PCR response is found to be relatively insensitive to source height, Appendix A. PCR motion forecasts use a height insensitive response that satisfies the first seven seconds of flight. For later times, the relative error will undoubtedly grow. The direction that the error takes depends on the type of structure. Motion forecasts for relatively tall, slim buildings like the PCR will in all likelihood be overestimated. In contrast, both the roofload and motion forecast for the Administration building will be underestimated when the forecast is constrained to use only the first 150 meters of Shuttle trajectory. As the Shuttle moves south, backscatter off the PPR south wall should nearly double and phase align the roofload on the Administration Building.

5.3 PCR Motion Simulations -

5.3.1 Particle Velocity - Figure 11 depicts particle velocity time histories for points on the upper and lower south PGHM rails assuming that the height insensitive building responses obtained in sounding tests will continue to apply when the Shuttle is above 150 meters. In this simulation the early rail motion is dominated by a lightly damped building sway in line with the Launch Mount. As the launch proceeds, the

## 5.0 MOTION FORECASTS

5.1 Motion Representation - After Backus (10), motion excited at a distance by a source acting at the origin of an elastic system can be expressed by:

$$u_k(x;t) = \sum_{n=1}^{\infty} \frac{1}{n!} G_{ki,j\cdots j_n}(x;t:0,0) \star M_{i,j\cdots j_n}(0;t)$$

For a small source the first term dominates (11), to give:

$$u_k(x;t) = G_{ki,j}(x;t:0,0) \star M_{ij}(0;t)$$

In turn, a simple center of pressure can be represented as the product of a function of time and a constant (12) to give, in this case:

$$M_{ij} = Y_{exp}(t) \cdot \alpha \cdot \delta_{ij} \qquad \delta_{ij}=0 \quad i \neq j \qquad \delta_{ij}=1 \quad i=j$$

Under these constraints, the component motion excited at a point within the PCR by an explosion over the Launch Mount is reduced to the temporal convolution of a source pressure with the response of a time invariant linear system:

$$u_k(PCR;t) = G(PCR;t:h,0) \star p_{exp}(t)$$

The motion excited by the moving rocket leads to a time dependent path. For

reverberation pattern excited by a source under 100 meters will continue to apply at higher altitudes. For a STS launch, our forecast best applies to times leading up to the OASPL maximum. The forecasted peak pressure in the band $0.3 < f < 30$ Hz for the face of the PCR is 164.4 ± 1.1 db. The expected SPL maximum for one second averaging is 155.8 ± 0.5 db, Figure 8. The corresponding SPL maximum for the same offset at KSC, free of the ground-cloud, is 148.7 db.

4.5.2 AB Roof - In like manner, we simulate pressure on the roof of the Administration Building over a sequence of launches, Figure 9. As for the face of the PPR, spectral shape is substantially altered by site unique reverberations, Figure 10.

Table 2 compares the results of a third octave analysis using 2.56 second samples around the OASPL maximum from one simulation with corresponding values obtained for 41B and a simulated launch at a flat-earth site for a surface observer offset of 761 meters. The OASPL for Mission 41B is 149 dB. The comparable flat-earth value using EOD wavelets in this simulation is 148.3 db. The flat-earth OASPL value is quite close to 6.4% model estimates (5). Pressure simulations for the roof of the Administration Building and the face of the PPR tend to be higher than those established at reverberation free sites. The disparity between pressures tends to grow at higher frequencies.

4.5 Launch Pressure Simulations - The mapping operator W(t) obtained from flat-earth measurements is now applied to pressure wavelets produced by 2.5 pound charges detonated over the Launch Mount:

$$p^{V23}_{STS}(r;t) = W(t) * p^{V23}_{exp}(r;t) * E(r;t \cdot N(0,1)$$

where: $p^{V23}_{exp}(r;t) = \emptyset_{V23}(r,h;t) * Y_{exp}(t)$ contains the site response and W(t) is defined by the operation:

$$Y_{STS}(t) = W(t) * Y_{exp}(t)$$

4.5.1 East Face of PPR - Shuttle launch pressure forecasts within the V23 station area differ markedly from pressures measured at flat-earth sites after allowance for boundary effects. Figure 6 shows a sequence of simulated launch pressures on the east face of the PPR that contain reverberations excited by shots detonated over the Launch Mount. The pressure on the east face of the PPR differs significantly from simulated or measured pressures for a flat-earth site at the same offset.

Reverberations encountered at Station V23 alter both the level and spectral shape of the load on the PPR. Figure 7 is the ratio between the pressure spectral level on the PPR with like values for a flat-earth site. Surface loads on the PPR are enhanced by as much as 14 db because of local boundary effects. The reverberation pattern is sensitive to source and observer location. Almost certainly, launch pressure at VAFB will continue to differ from ESC for times well after the Shuttle has cleared the Launch Mount.

Pressure time histories for simulated launches assume the

spectra produced by this explosion into STS launch pressure is given in Figure 3 with:

$$\left\{ \frac{PSD_{STS}(a_s, f)}{ESD_{exp}(a_s, f) \cdot 1/T} \right\}^{\frac{1}{2}}$$

Phase is specified by demanding that the operator be realizable and of minimum phase (9).

4.4 Simulation Source Error - If only to provide a check, we simulate a STS launch for a flat-earth site based on a 2.5 pound shot wavelet measured at the VAFB EOD Test Range using:

$$p^{FE}_{STS}(r;t) = W(t) * p^{FE}_{exp}(r;t) * E(r;t) \cdot N(0,1)$$

Simulated launch pressure is plotted directly above Mission 41B pressure measurements taken 291 meters southwest of Pad 39A, Figure 4. As can be readily seen, broadband surface pressures for actual and simulated launches look much alike. The main difference between the two lies in a change in spectral content that occurs over time for the actual launch. To show this, we construct a sequence of bandwidth limited pressure envelopes for the launch of 41B, Figure 5. The low frequency envelope for an actual launch is more persistent than allowed by the broadband envelope. Also, the low frequency portion of the ignition pulse for an actual launch is less attenuated by pad structure and, as noted in other studies, the true plume spectrum drifts to lower frequencies as the rocket climbs to altitude (2,7). Looking ahead, our simulations should tend to moderately underdrive low frequency (< 5 Hz), lowly damped (< 10%) structures such as the PCP.

for launch induced surface pressure at points not blanketed by the exhaust cloud for offsets of $250 < r < 350$ meters over a flat, open area like KSC.

4.2.2 Explosion Source - In much the same way, surface pressure generated by an atmospheric explosion satisfies:

$$p_{exp}(a_s;t) = W(a_s,h;t) * Y_{exp}(t) * \delta(t)$$

with extrapolations about $a_s$ over a flat-earth site in the range of interest again governed by small source, far-field, spherical acoustics:

$$p_{exp}^{FF}(r;t) = W_{FE}(a_s,h;t) * f_{exp}(t) * \delta(t) \cdot \frac{a_s \cdot e^{ik(r-a_s)}}{(a_s + (c_\alpha/c)^2 (r-a_s))}$$

In these representations, differences between explosion and launch generated surface pressures are separated into purely site and source attributes. Source differences can then be directly estimated from measurements at sites with like boundary conditions.

4.3 Source Mapping Operator - We seek an operator W(t) that maps an explosion pressure into an equivalent plume source for common boundary conditions and source-observer geometry:

$$p_{exp}(a_s;t) * W(t) = p_{STS}(a_s;t)$$

Figure 2 is a standard form surface spectrum obtained for Mission 41B using observations in the clear, 290 meters SSW of Pad 39A (2). Included in the figure is the spectrum of the wavelet produced by a 2.5 pound explosive charge for the same offset and averaging time at a flat-earth site, see Appendix B. The amplitude needed to convert surface pressure

FIGURES PAGE


| | | |
|---|---|---|
| 1 | V23 Station Elements | 22 |
| 2 | Standard Spectrum: Mission 41B | 23 |
| 3 | Mapping Operator Amplitude | 24 |
| 4 | Launch Surface Pressure For A Flat-Earth Site | 25 |
| 5 | STS Envelope Characteristics | 26 |
| 6 | Simulated Pressure For Shuttle Launches. | 27 |
| 7 | Spectral Ratio for PPR with a Flat-Earth Site | 28 |
| 8 | Pressure Level Forecast For Multiple Launches | 29 |
| 9 | AB Roof Pressure Forecast For Multiple Launches | 30 |
| 10 | Spectral Ratio For AB Roofload with a Flat-Earth Site | 31 |
| 11 | Velocity Time Histories: PCR - South PGHM Rails | 32 |
| 12 | Displacement Time Histories: PCR - South PGHM Rails | 33 |
| 13 | Acceleration Time Histories: PCR - South PGHM Rails | 34 |
| 14 | Acceleration Spectra Estimates: PCR | 35 |
| 15 | Pseudo-velocity Response Spectra: PCR | 36 |
| 16 | Acceleration Time Histories: AB | 37 |
| 17 | Acceleration Spectra: AB | 38 |
| 18 | Pseudo-velocity Response Spectra: AB | 39 |
| 19 | Displacement Maxima Distribution: PGHM Rail | 40 |
| 20 | Distribution of Absolute Displacement Maxima: PCR | 41 |
| 21 | Peak PCR Displacements For Multiple Launches | 42 |
| 22 | Distribution of Absolute Displacement Maxima: OFS | 43 |

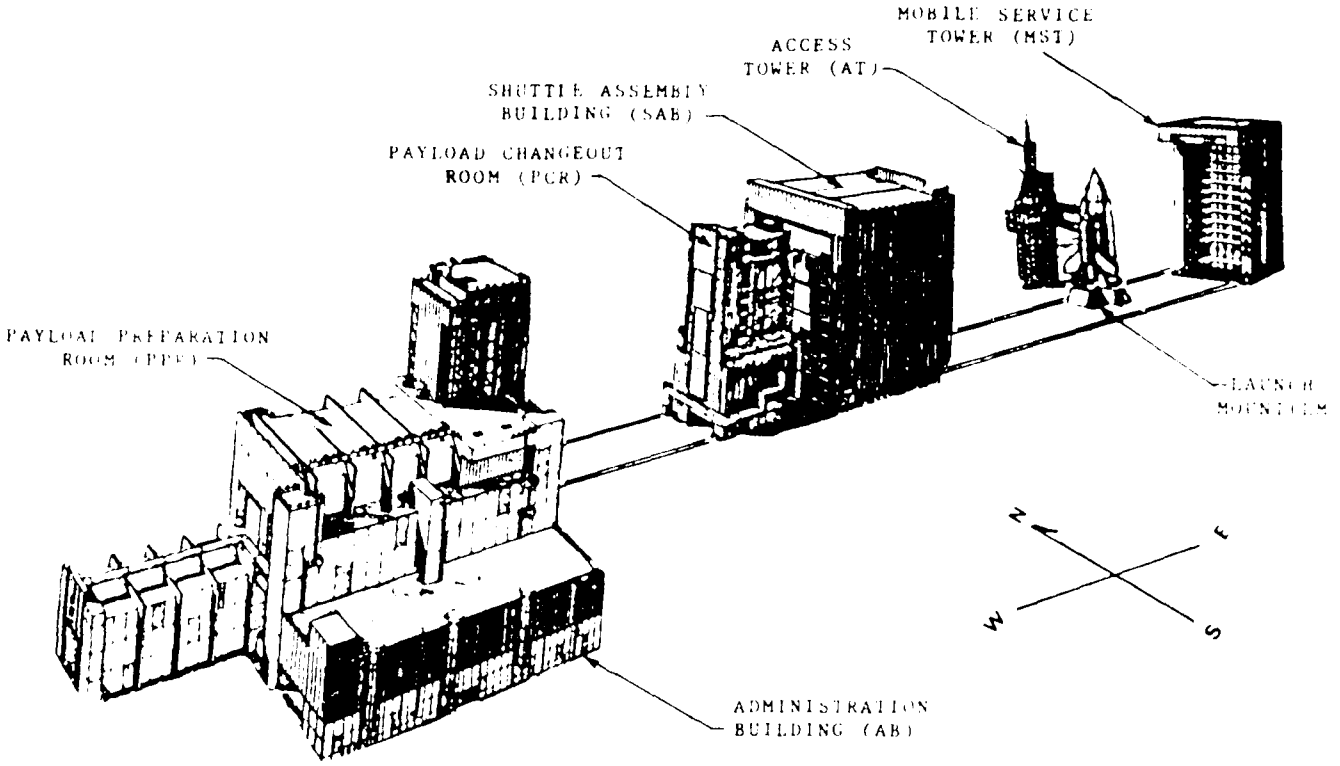


V 23 STATION ELEMENTS

Figure 1

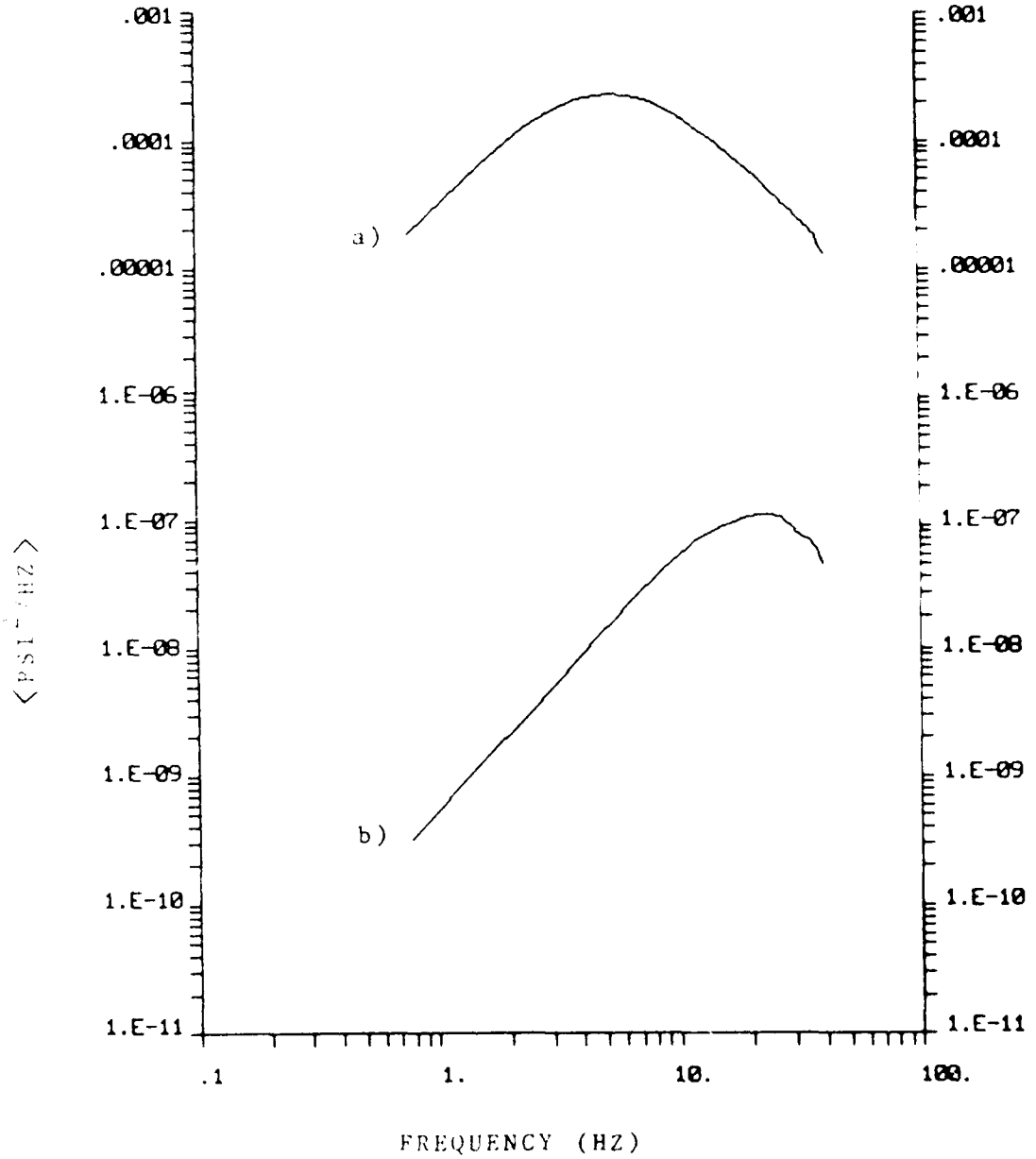


a) STS: Power Spectrum

b) 2.5 Pound Charge: Energy Spectrum/Time

STANDARD SPECTRUM: MISSION 41B

Figure 2

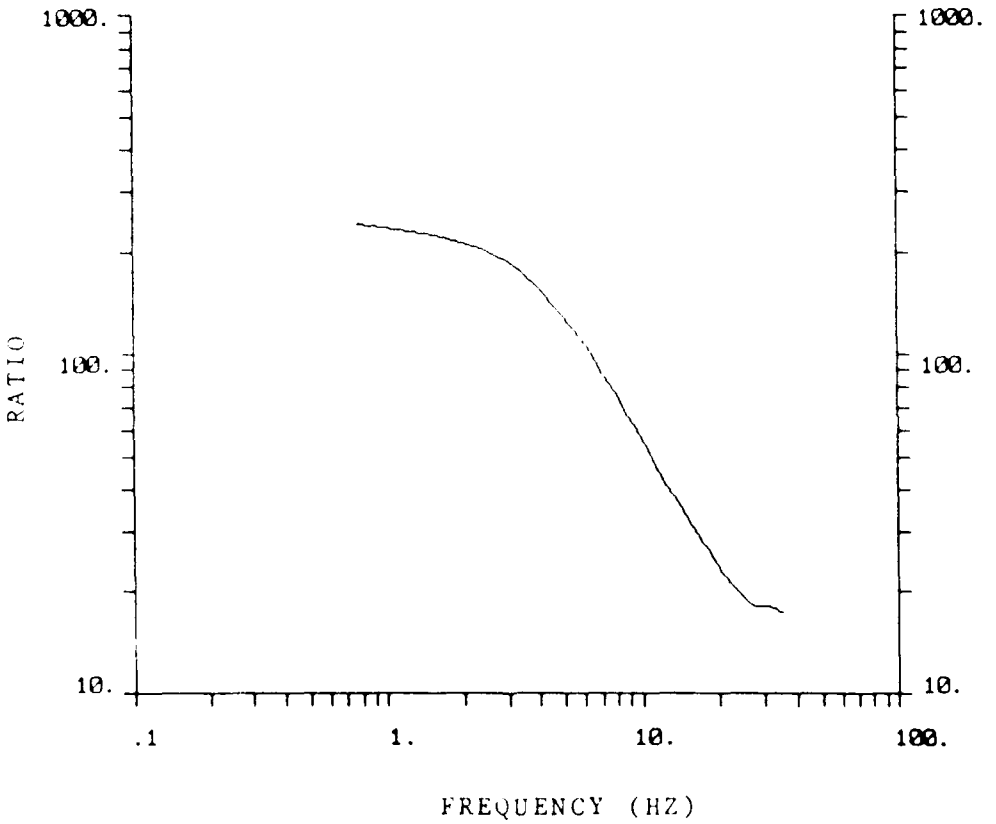


MAPPING OPERATOR AMPLITUDE

Figure 3

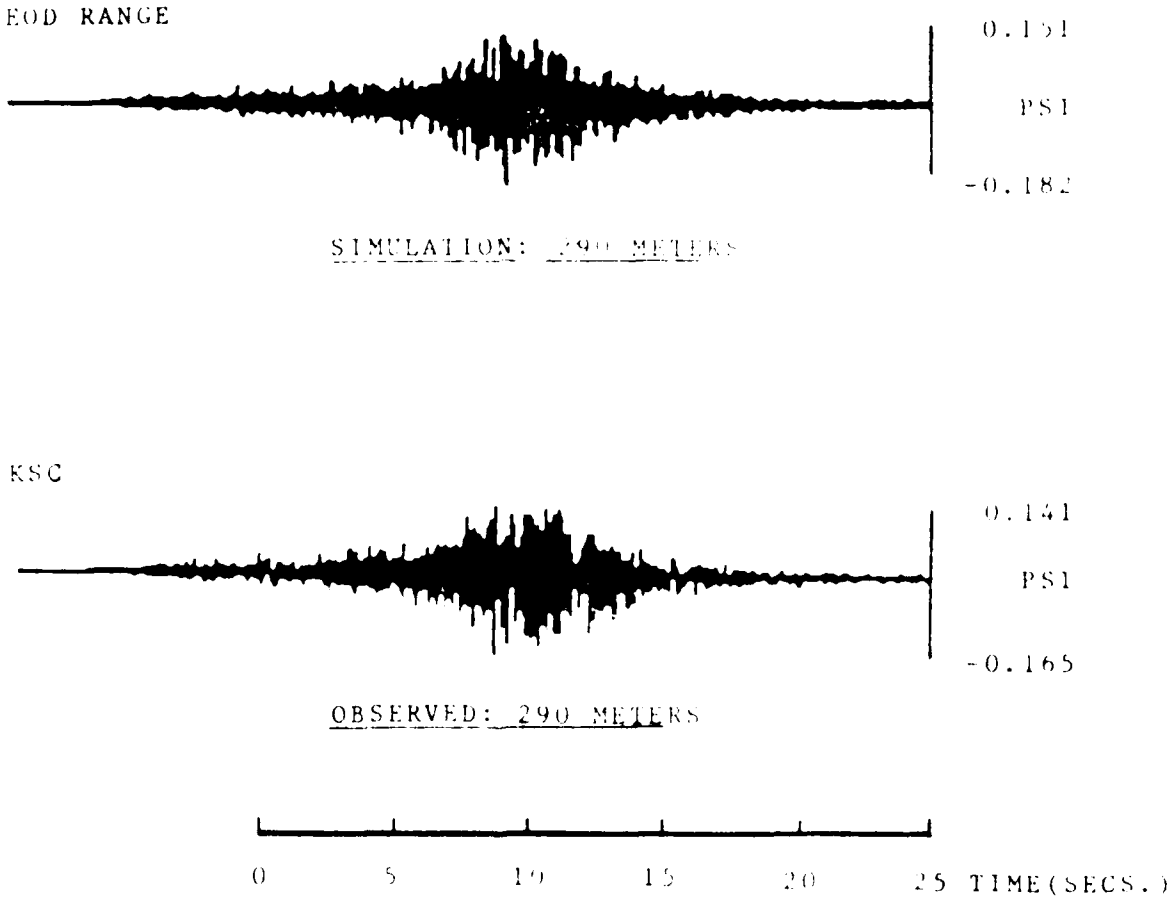


LAUNCH SURFACE PRESSURE FOR A FLAT-EARTH SITE

Figure 4

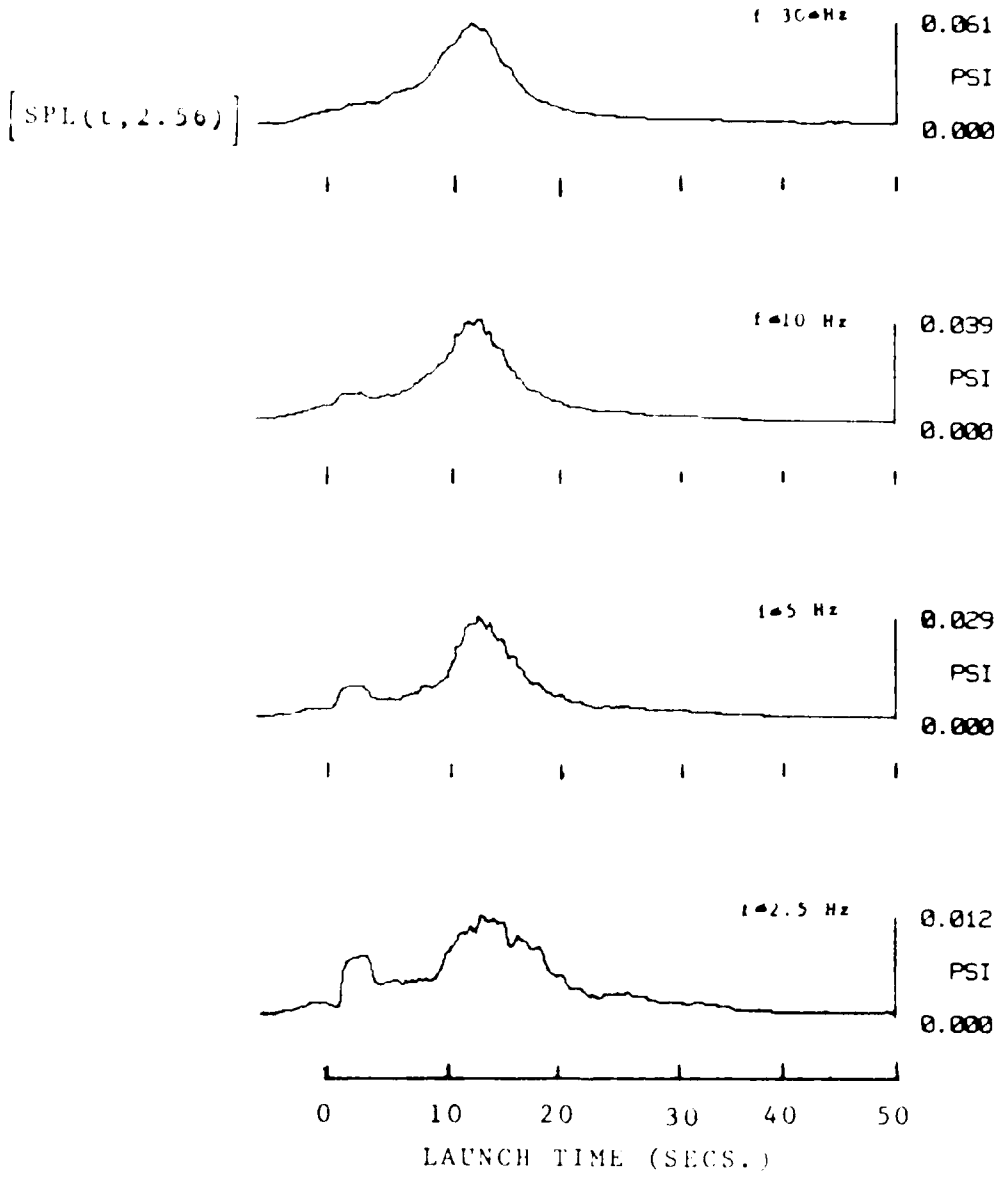


Offset= 290 METERS

STS ENVELOPE CHARACTERISTICS
MISSION 41B

Figure 5

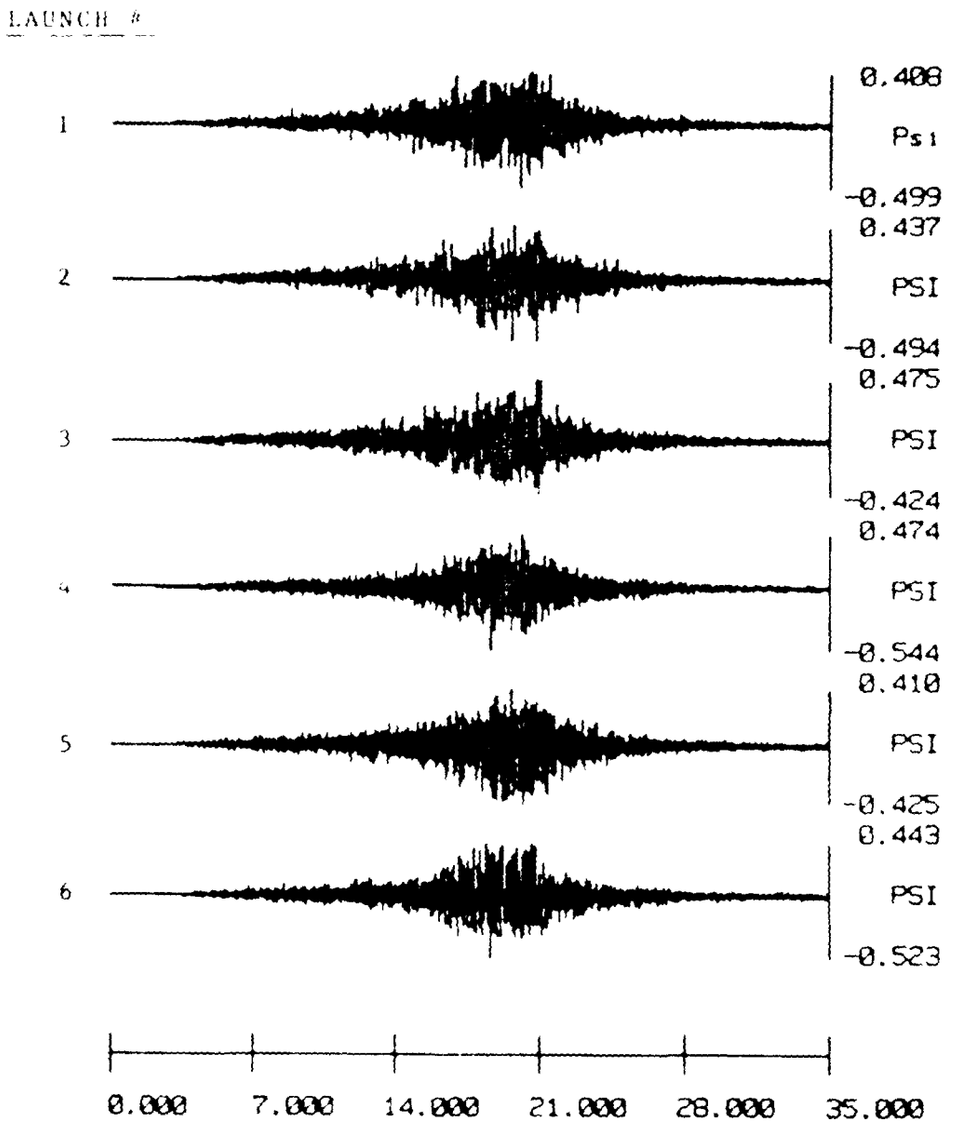


SIMULATED PRESSURE FOR SHUTTLE LAUNCHES:

(EAST FACE OF VPR)

Figure 6

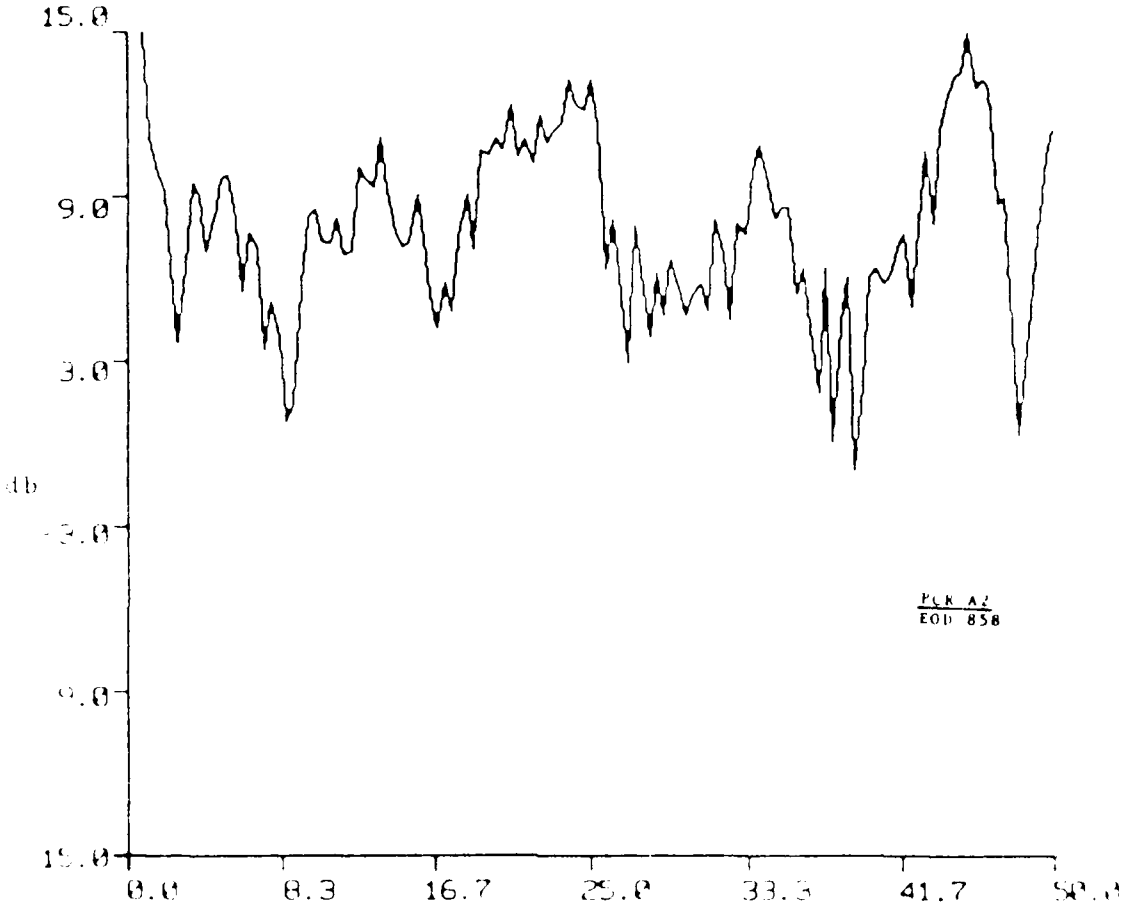


SPECTRAL RATIO FOR PPR WITH A FLAT-EARTH SITE

Figure 7

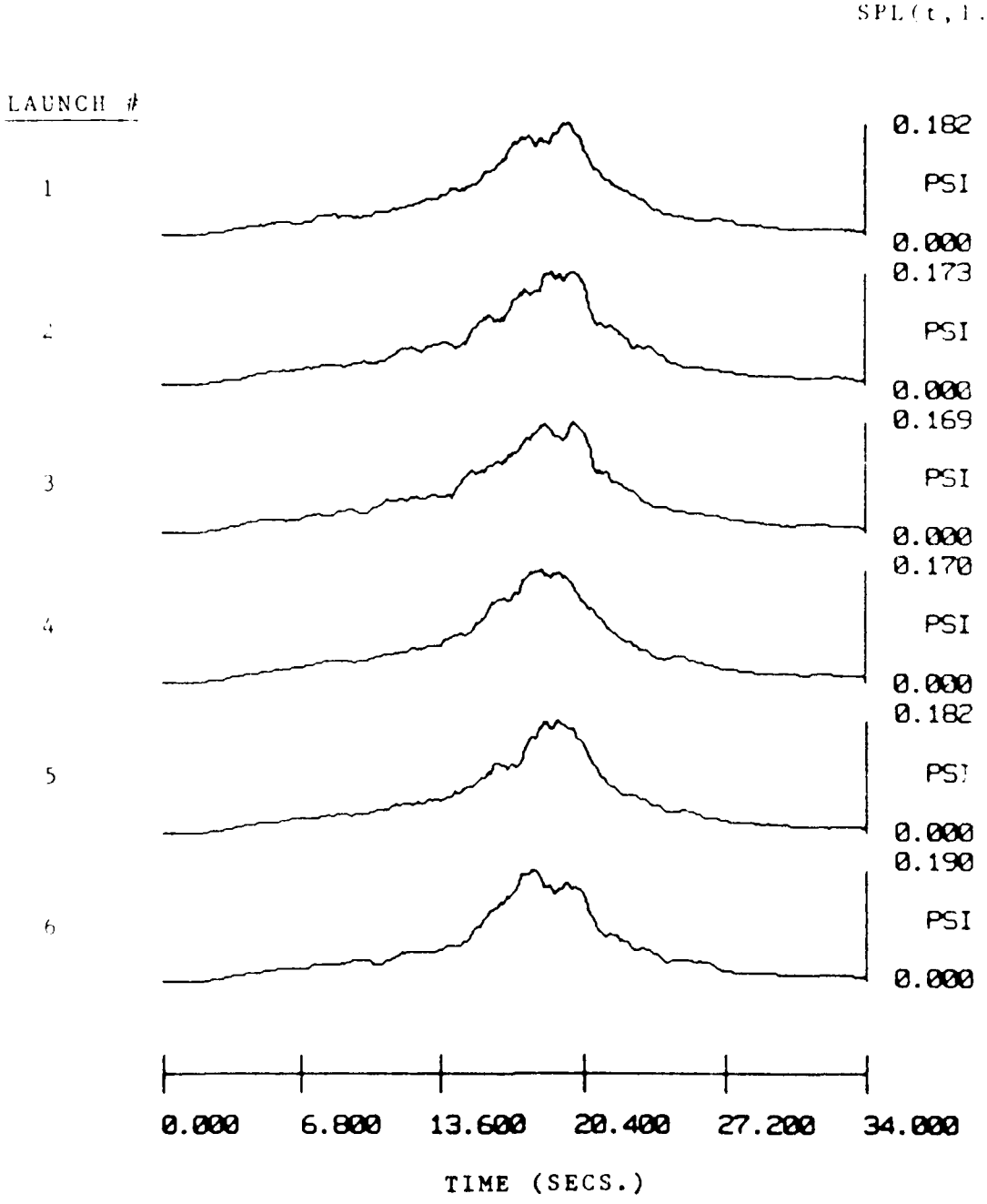


PRESSURE LEVEL FORECAST FOR MULTIPLE LAUNCHES
(EAST FACE OF PPR)

Figure 8

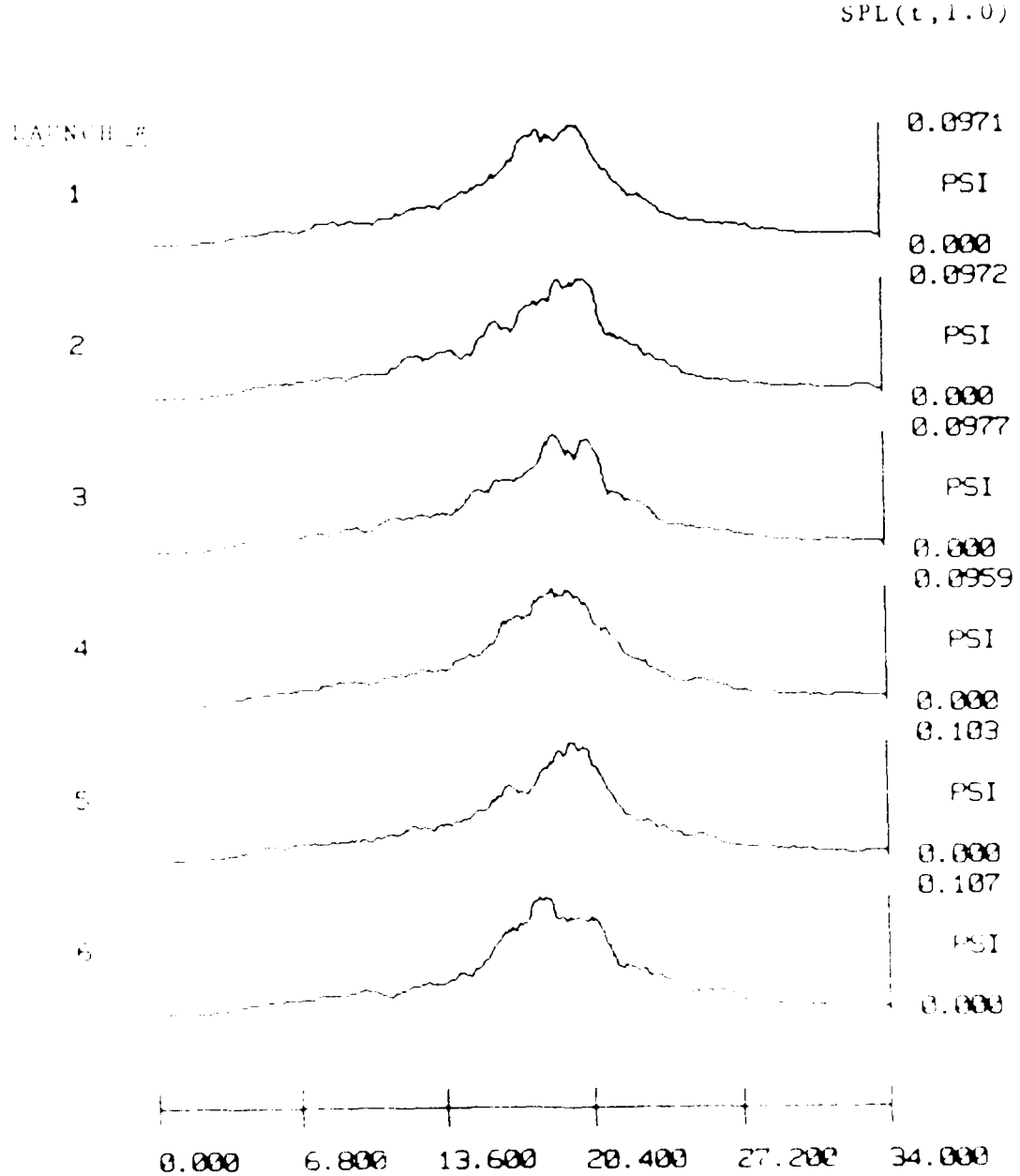


A2 BOOT PRESSURE FORECAST FOR MULTIPLE LAUNCHES

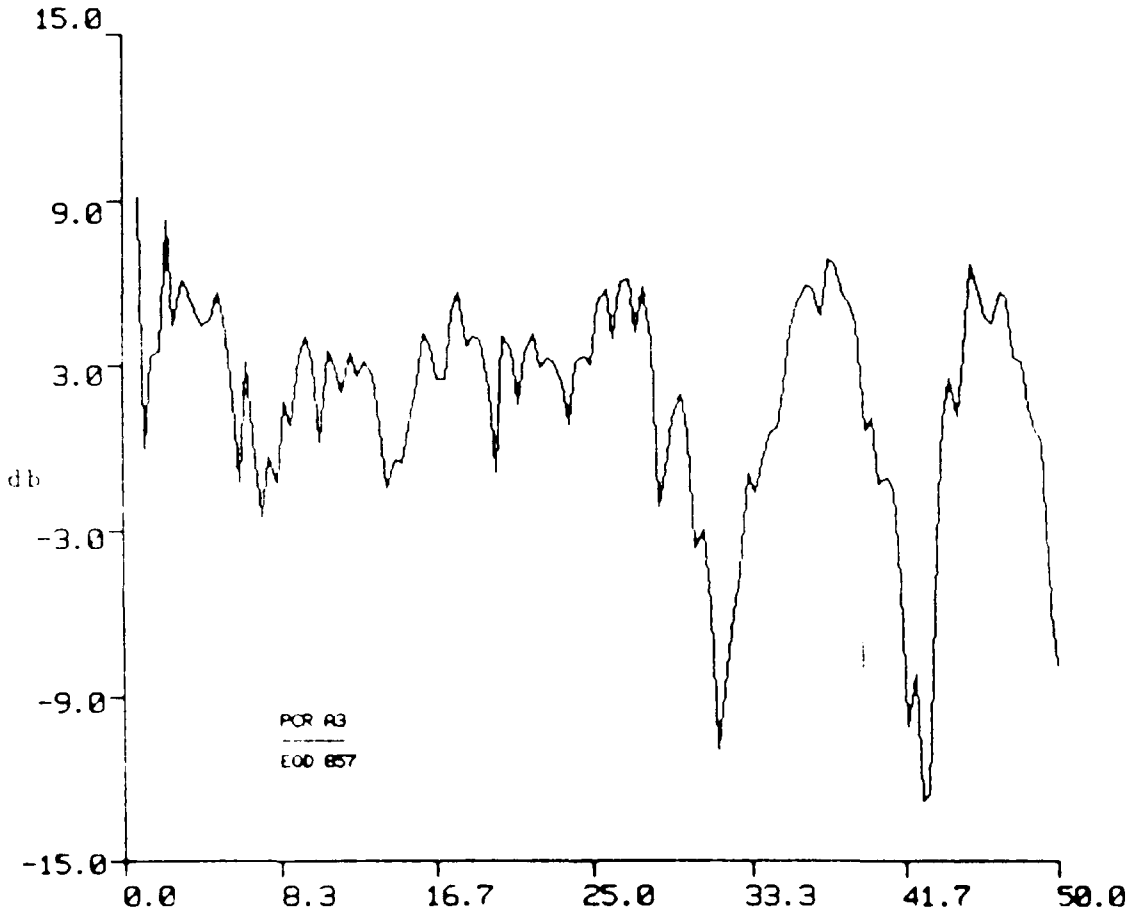


SPECTRAL RATIO FOR AB ROOFLOAD WITH A FLAT-EARTH SITE

Figure 10

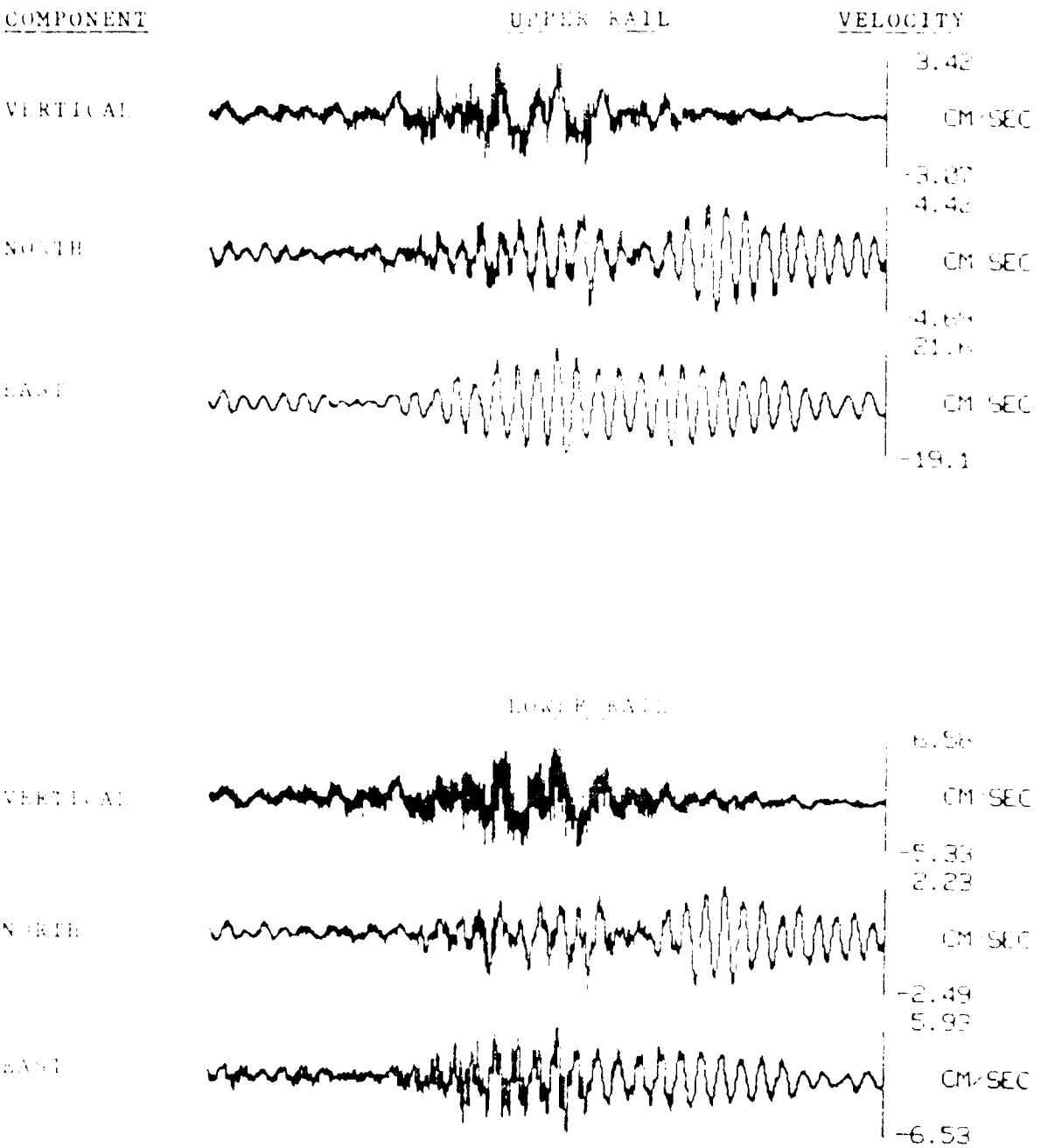


VELOCITY TIME HISTORIES: PCR, SOUTH PGHM RAILS

SIMULATION NO. 5.A1

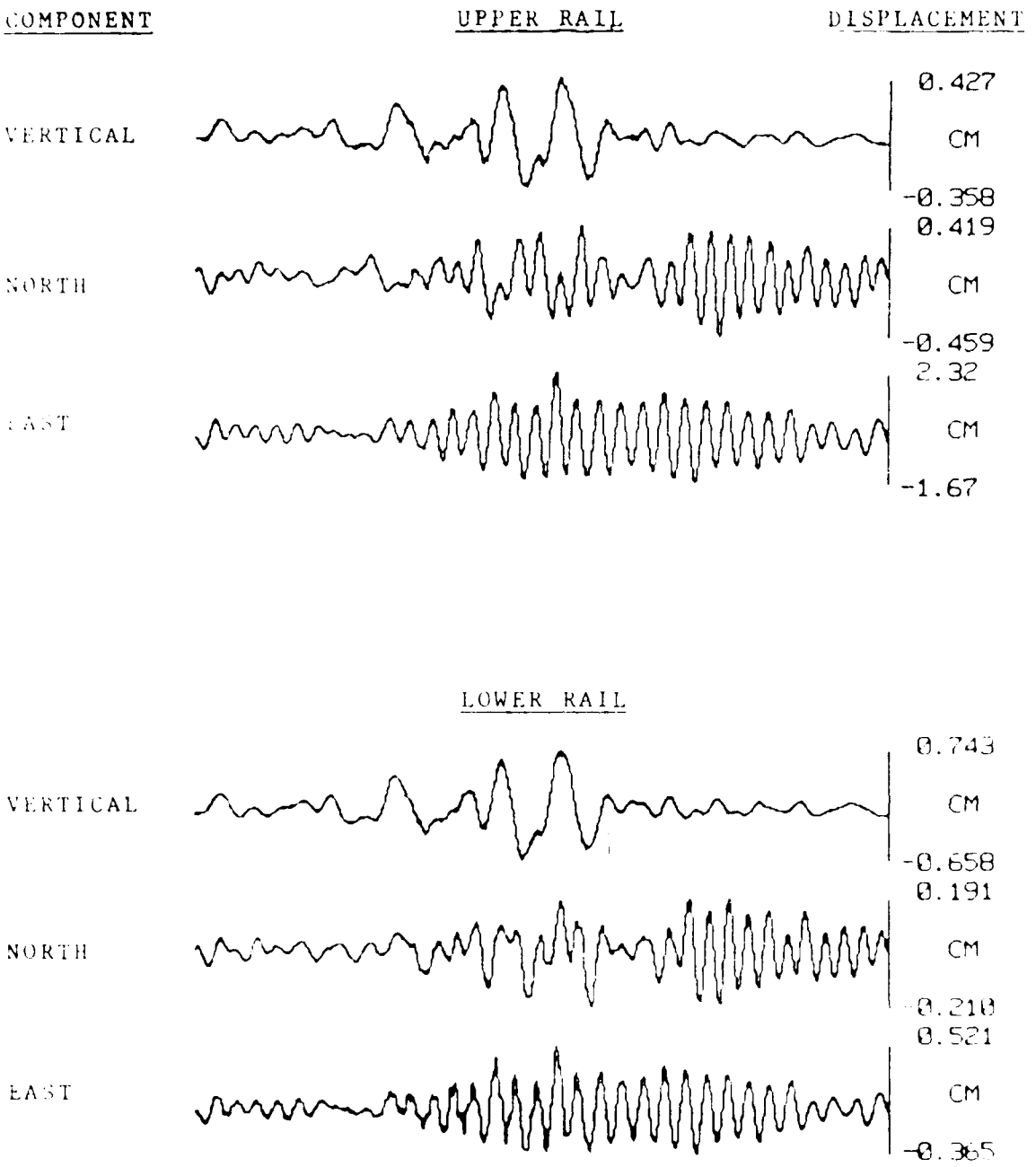


DISPLACEMENT TIME HISTORIES: PCR, SOUTH PGHM RAILS

SIMULATION NO. 6;A1

Figure 12

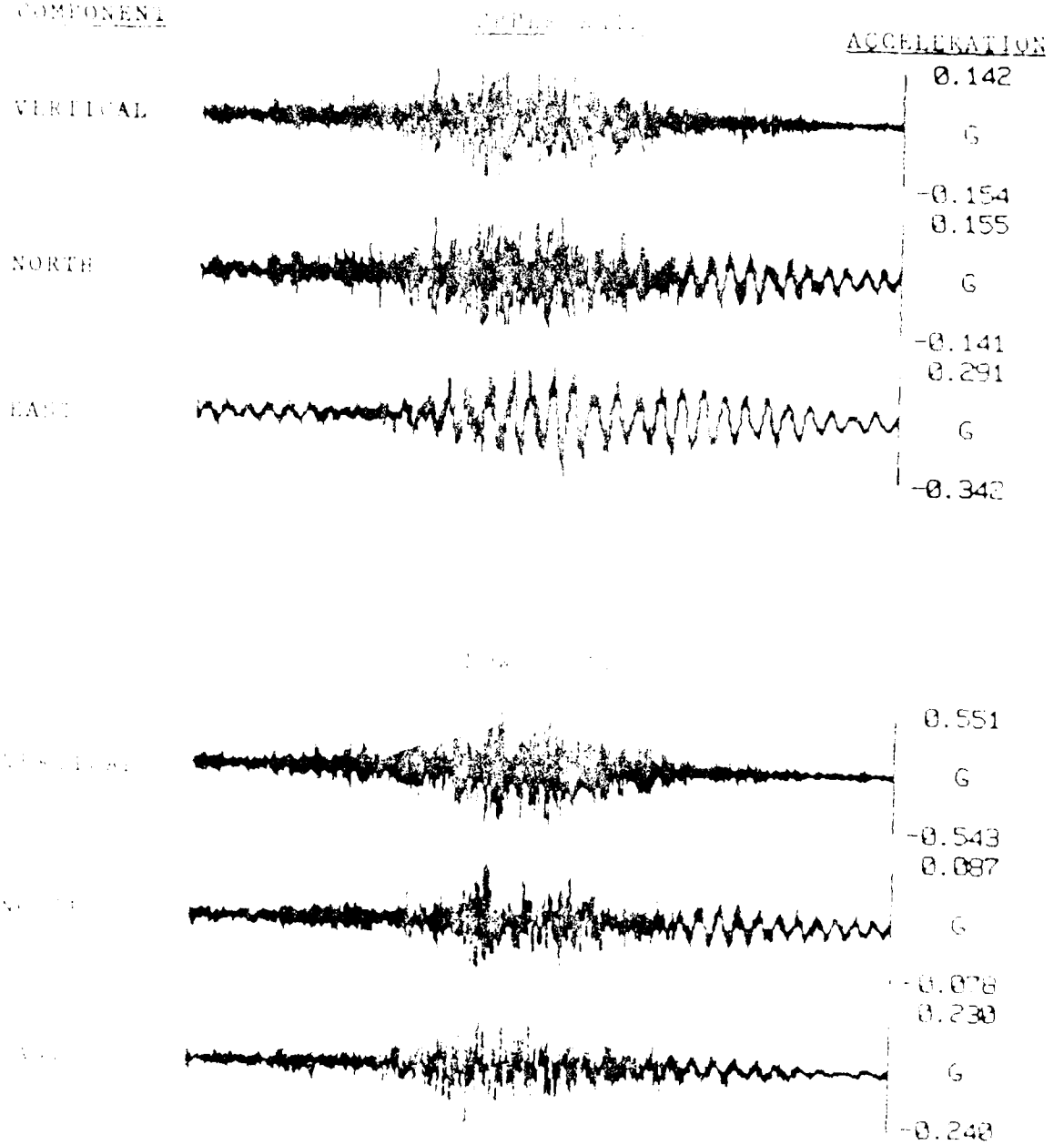
COMPONENT
ACCELERATION
VERTICAL
0.142
G
-0.154
NORTH
0.155
G
-0.141
EAST
0.291
G
-0.342
0.551
G
-0.543
0.087
G
-0.078
0.230
G
-0.248
BANDPASS
0.3<f<10.0 HZ

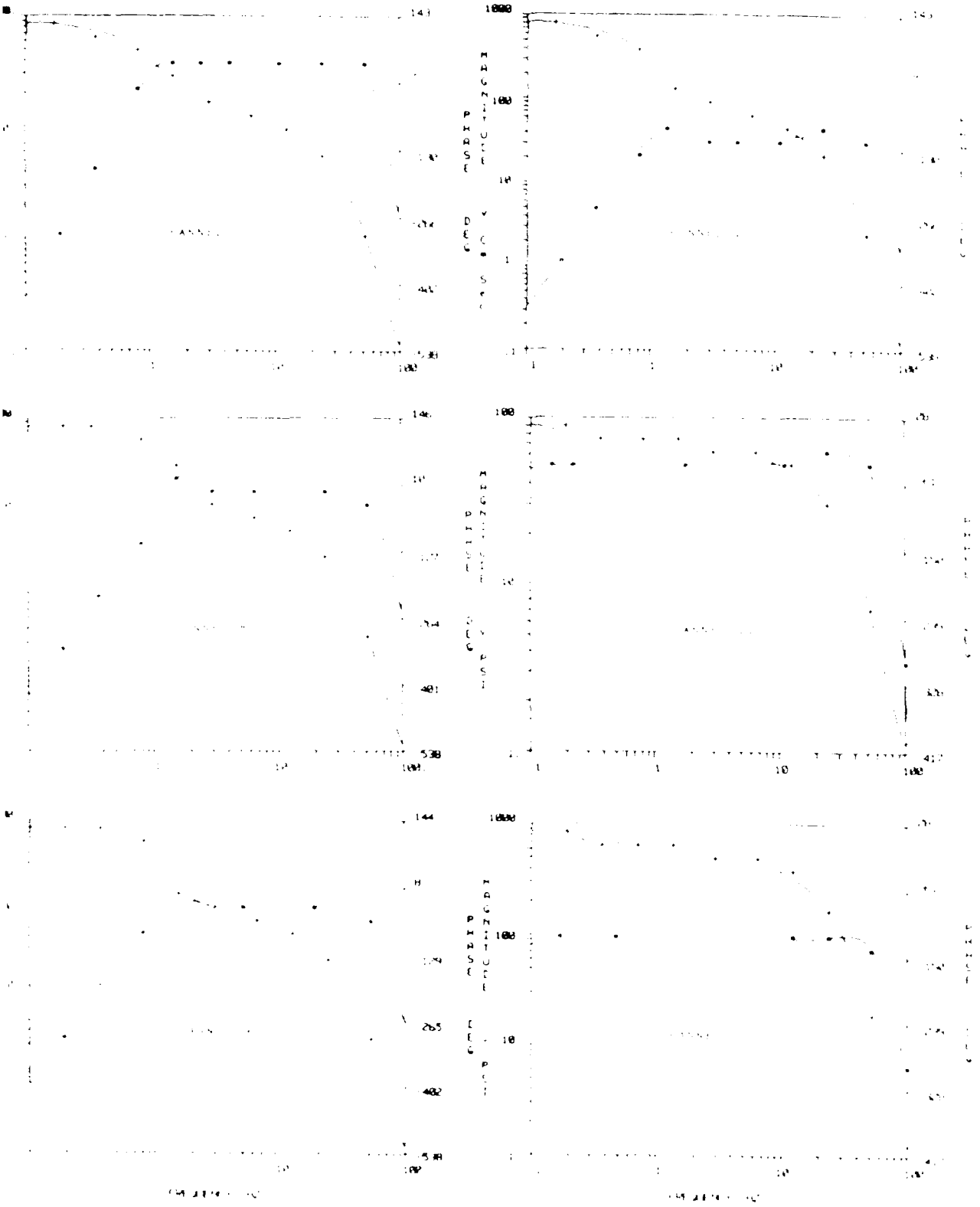

Figure 2A

★ Magnitude
+ Phase

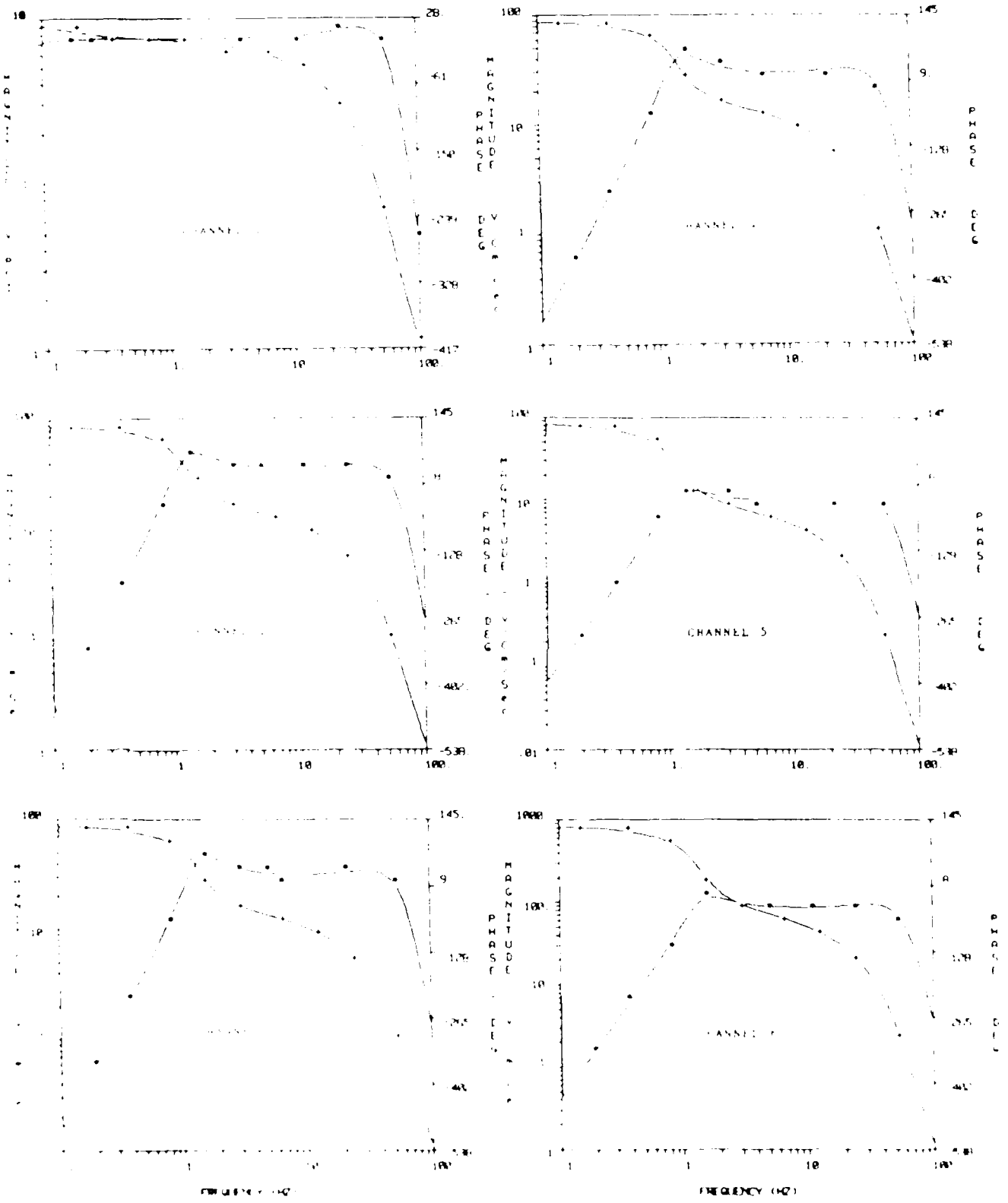


CHANNEL RESPONSES (CHANNELS 1-6 INCLUSIVE)

Figure 1A

★ Magnitude
+ Phase

TABLE 1A SOUNDING TESTS
CHANNEL IDENTIFICATION

| | MEASUREMENT | FACILITY | LOCATION |
|---|---|---|---|
| | Pressure | V23 | 50 meters west of LM |
| | Seismic X | PCR | South PCHM Lower Rail |
| | N | | |
| | E | | |
| | Seismic Z | PCR | South PCHM Upper Rail |
| | N | | |
| | L | | |
| | Seismic Z | AF | OFS Floor |
| | N | | |
| | E | | |
| | Pressure | PPR | East Face PPR |
| | Pressure | AL | Roof |

Shot Elevation
[illegible]
[illegible]
[illegible]

Charge Weight: 2.5 lbs
15 m above LM
45 m above LM
60 m above LM

Individual channel responses for these tests are given in Figures 1A and 2A. Channel scale factors are ultimately traceable to a force produced by a proof mass, or a pressure developed by a column of water of known height. Noise in these tests is dominated by the ambient conditions at shot time. Hardware noise is inconsequential (1,2).

Measured wavelets produced by 2.5 pound charges detonated 15, 45 and 60 meters above the Launch Mount are given in Figures 3A and 4A. The pressure and seismic wavelets establish site specific responses to acoustics emitted from 3 points along the STS trajectory and incident on 5 locations of interest to SATAF.

APPENDIX A: THE SOUNDING PROGRAM

The sounding program called for measuring pressures and motions produced by small charges detonated over the Launch Mount. The effort was one of a series of steps to upgrade forecasts of the vibro-acoustic environment for STS launches at VAFB. The V23 sounding program was planned in two segments. The first phase called for a limited effort to develop a factual base to tightly define and schedule a larger follow-on "production" effort that would minimally impact other site activities.

In April, 1984 SAIAF reconsidered its need to conduct the second phase effort; the proposed work was cancelled in August. As a consequence, the current study must be restricted to those points covered by the March tests.

On the morning of 17 March, 1984, seven charges were detonated over the Launch Mount with the V23 structures in launch configuration. The SAB roof and wall panels were not completely in place for these tests. Installation of the remaining panels should intensify reverberations.

In these tests, shot elevations were limited to 60 meters by the maximum possible height of a suspension line strung between the MST and [illegible]. Higher source elevations had been planned using a tethered balloon, but the provision to suspend charges from a ballon was dropped after a number of aborted launches.

Measurements were taken by an element of the AFGL Geophysical Data Acquisition System (GDAS) (14). As configured for the March 17 test, GDAS supported 6 seismic and 3 pressure measurements, see Table 17. Channel [illegible] were determined by analyzing transients excited by a step input with the system in place just before and after the shot sequence.

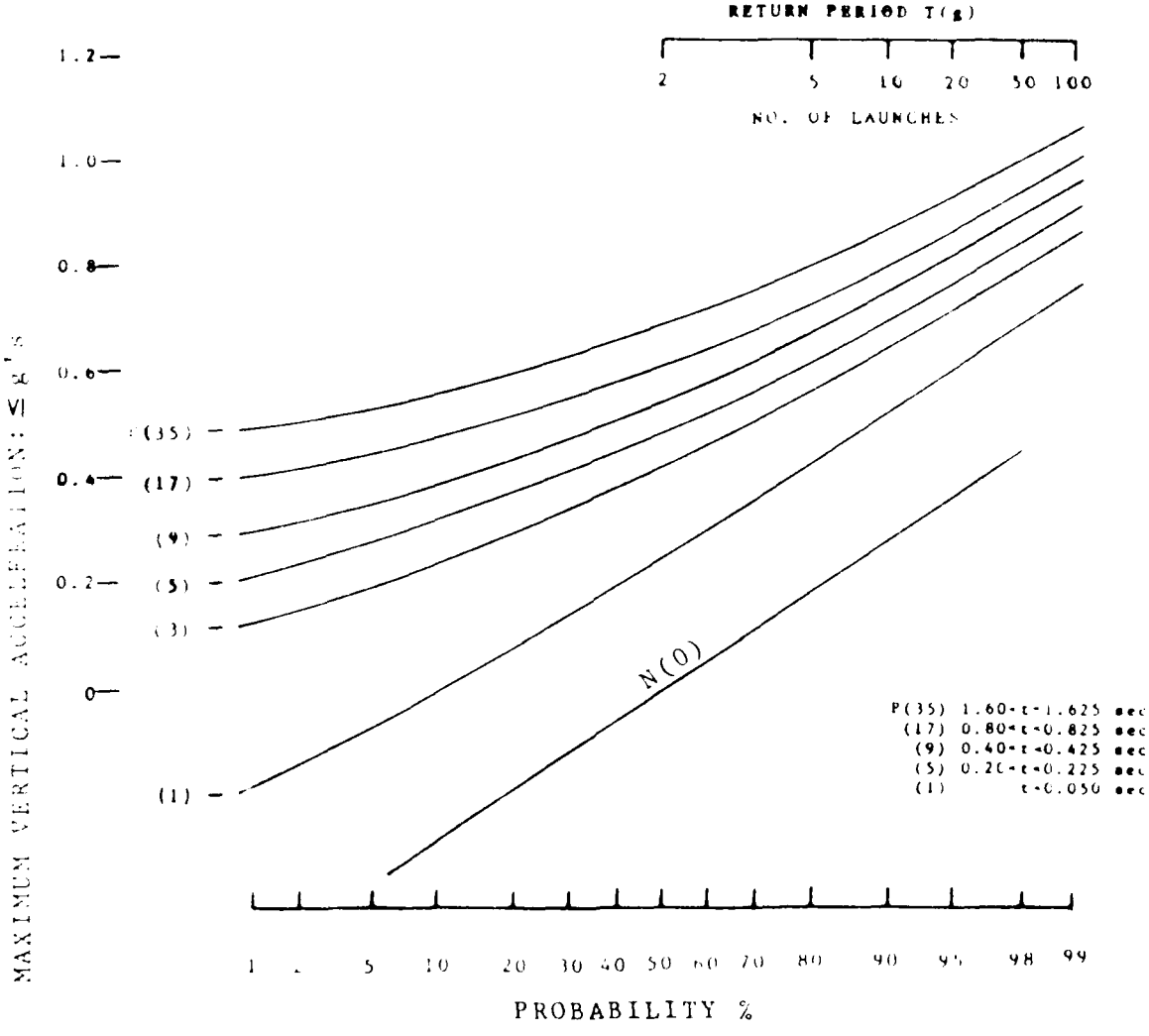


DISTRIBUTION OF ABSOLUTE ACCELERATION MAXIMA:OFS

Figure 22

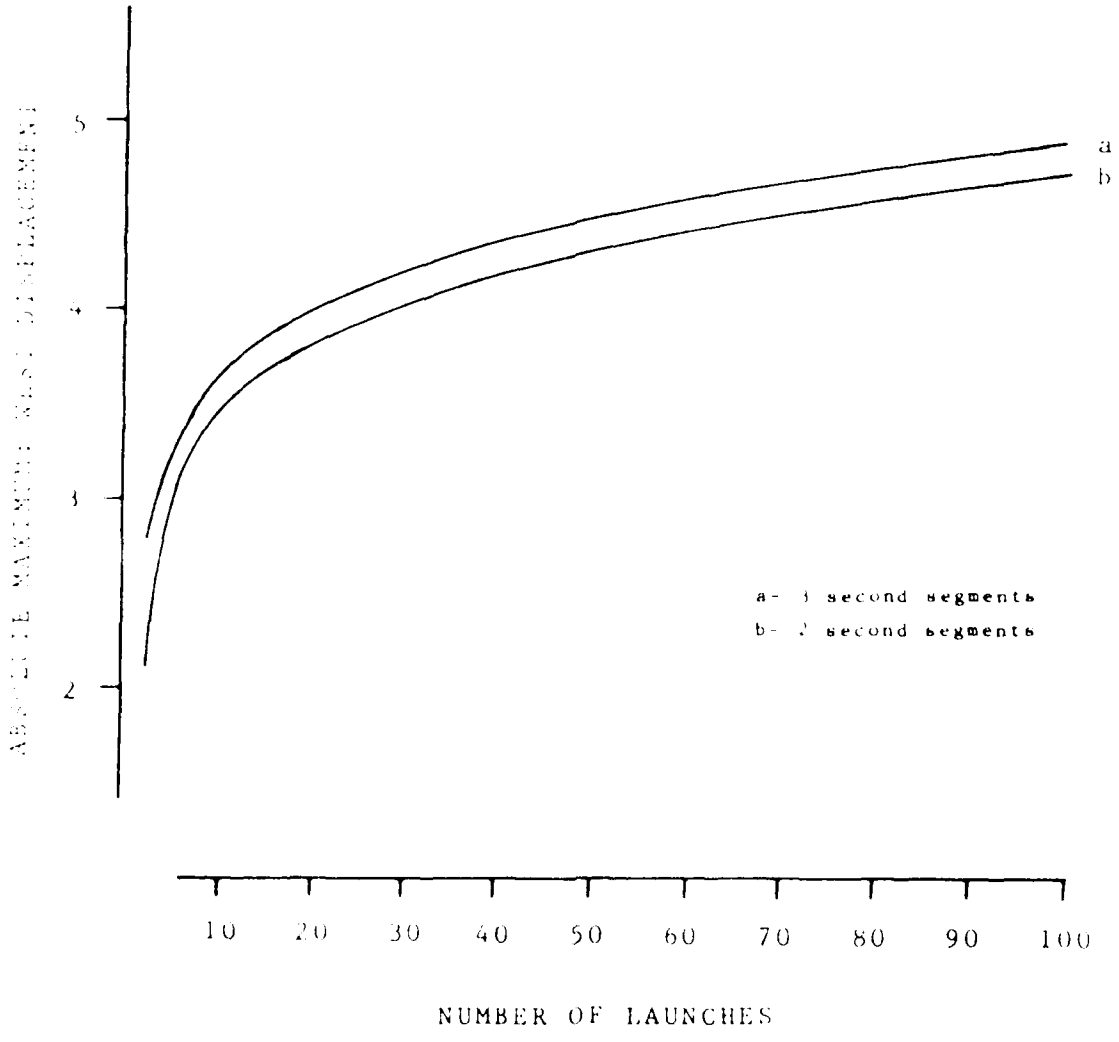


PEAK PCR DISPLACEMENTS FOR MULTIPLE LAUNCHES

Figure 21

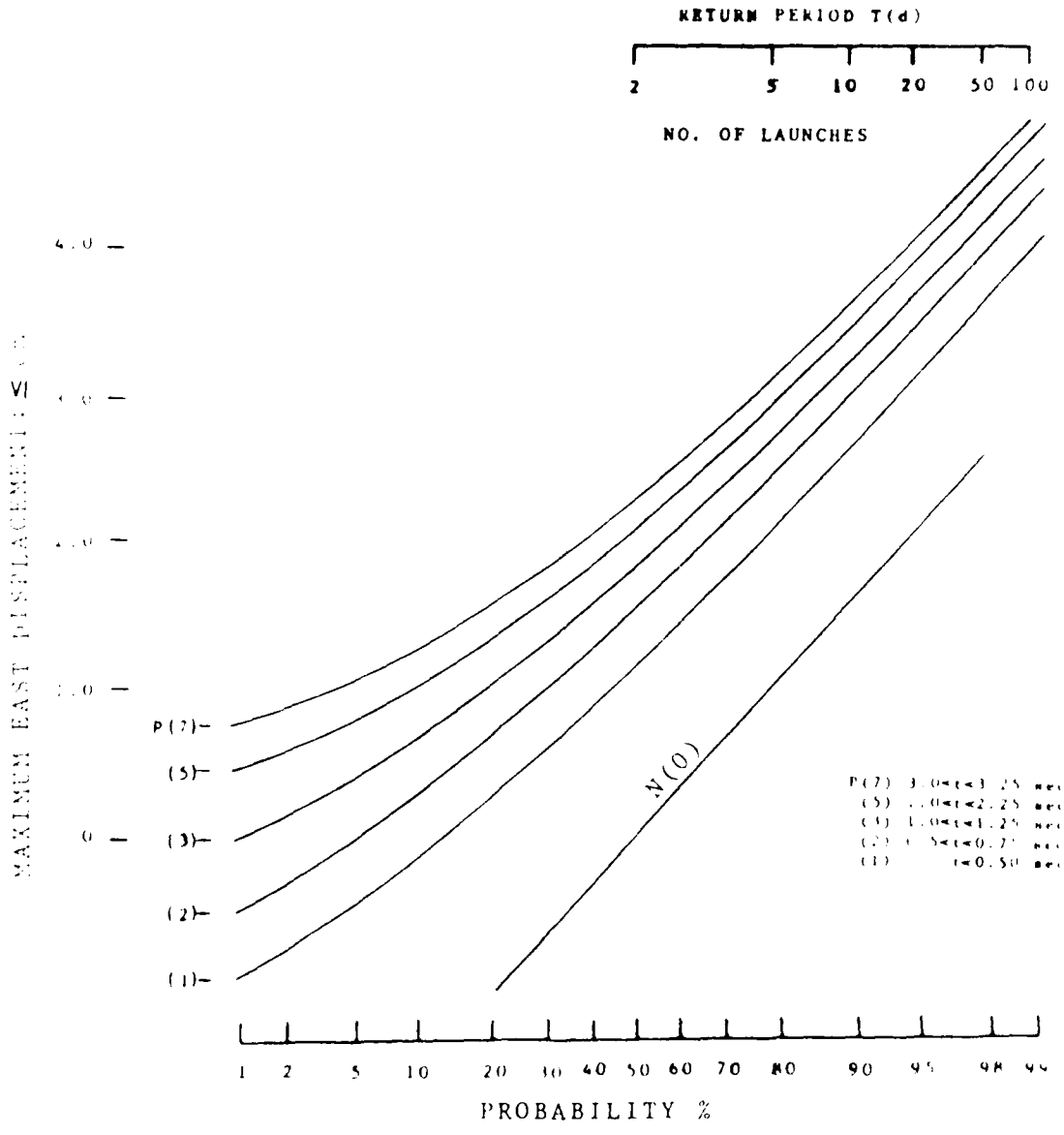


DISTRIBUTION OF ABSOLUTE DISPLACEMENT MAXIMA: PCR

Figure 20

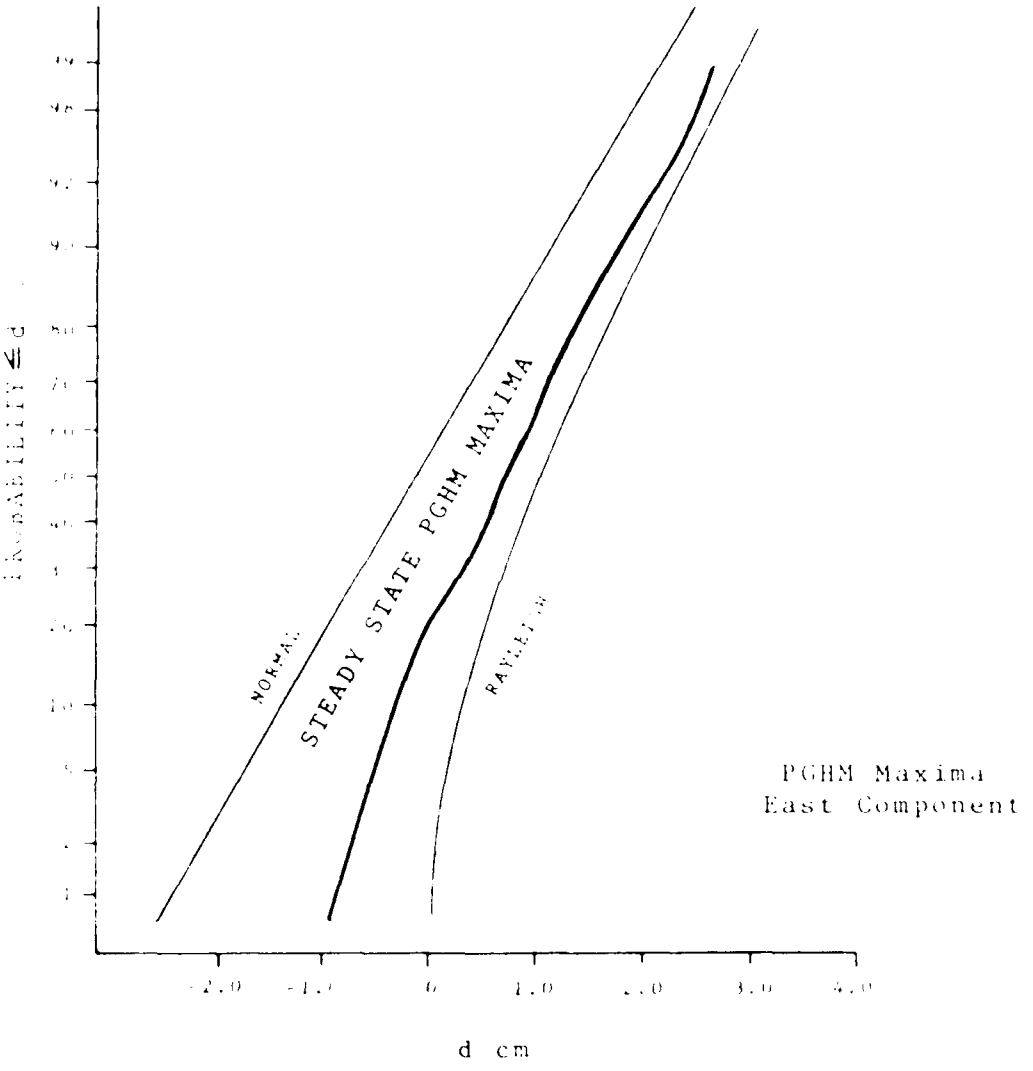


DISPLACEMENT MAXIMA DISTRIBUTION: PGHM RAIL

Figure 19

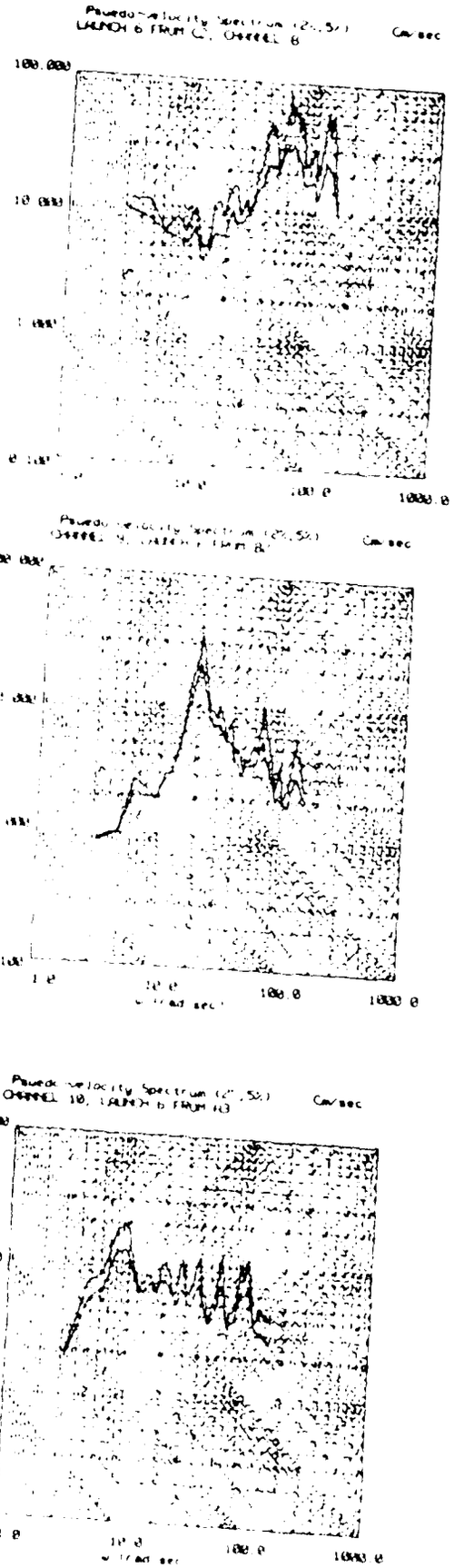

PSEUDO-VELOCITY RESPONSE SPECTRA: AB

Figure 18

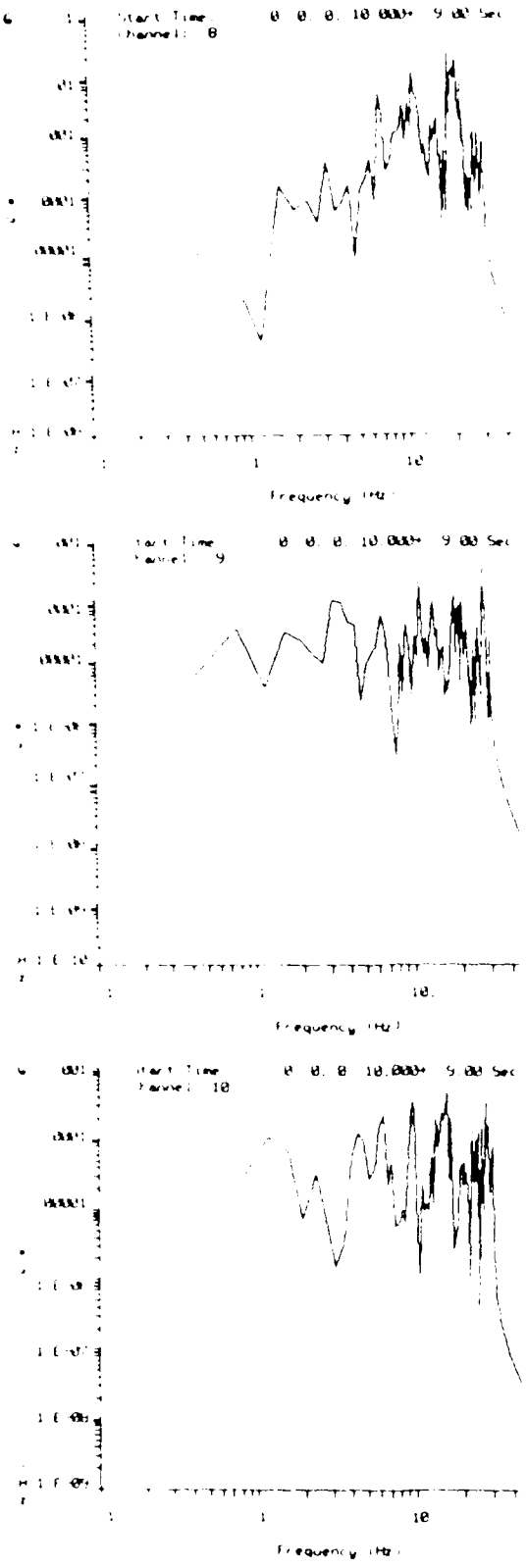

ACCELERATION SPECTRA: AB

Figure 17

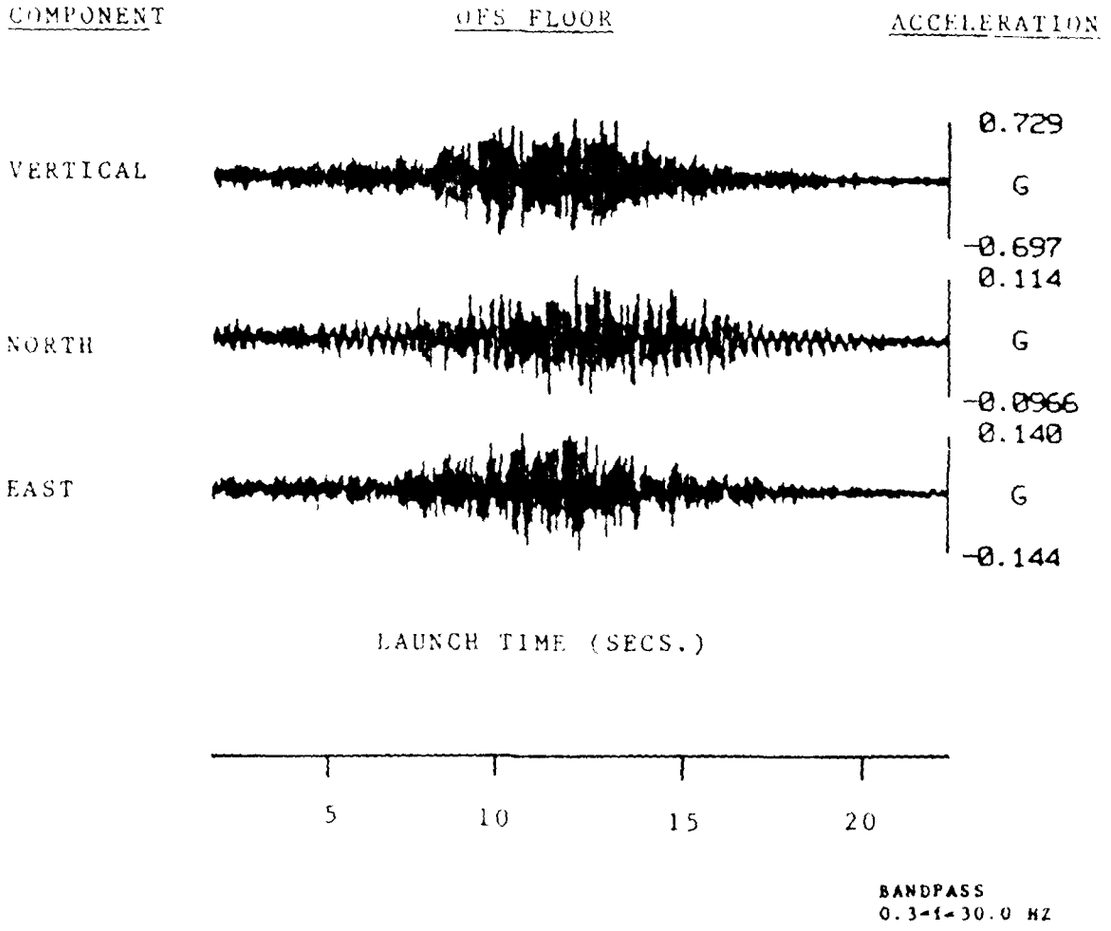


ACCELERATION TIME HISTORIES: AB

SIMULATION NO. 6;A3

Figure 16

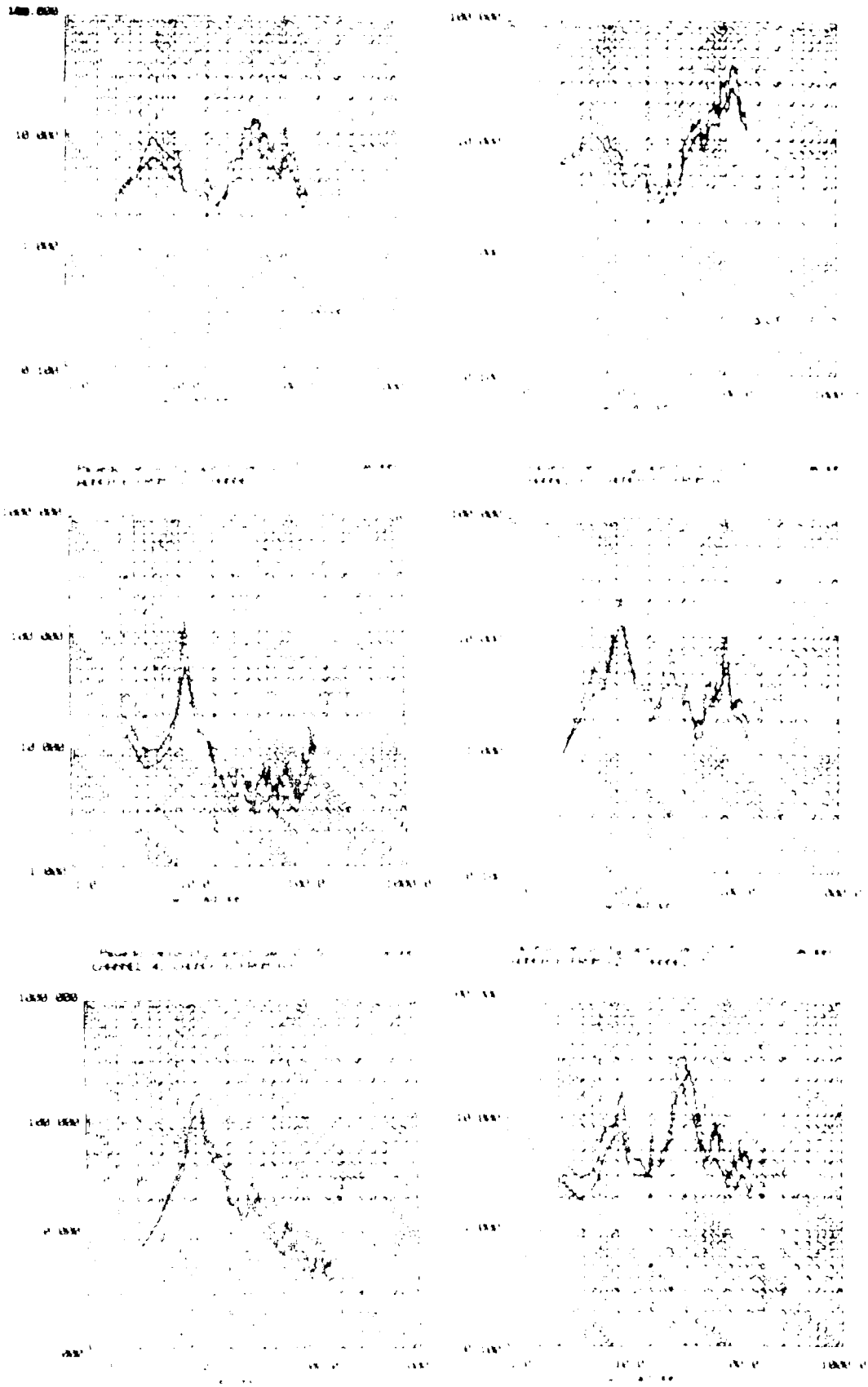

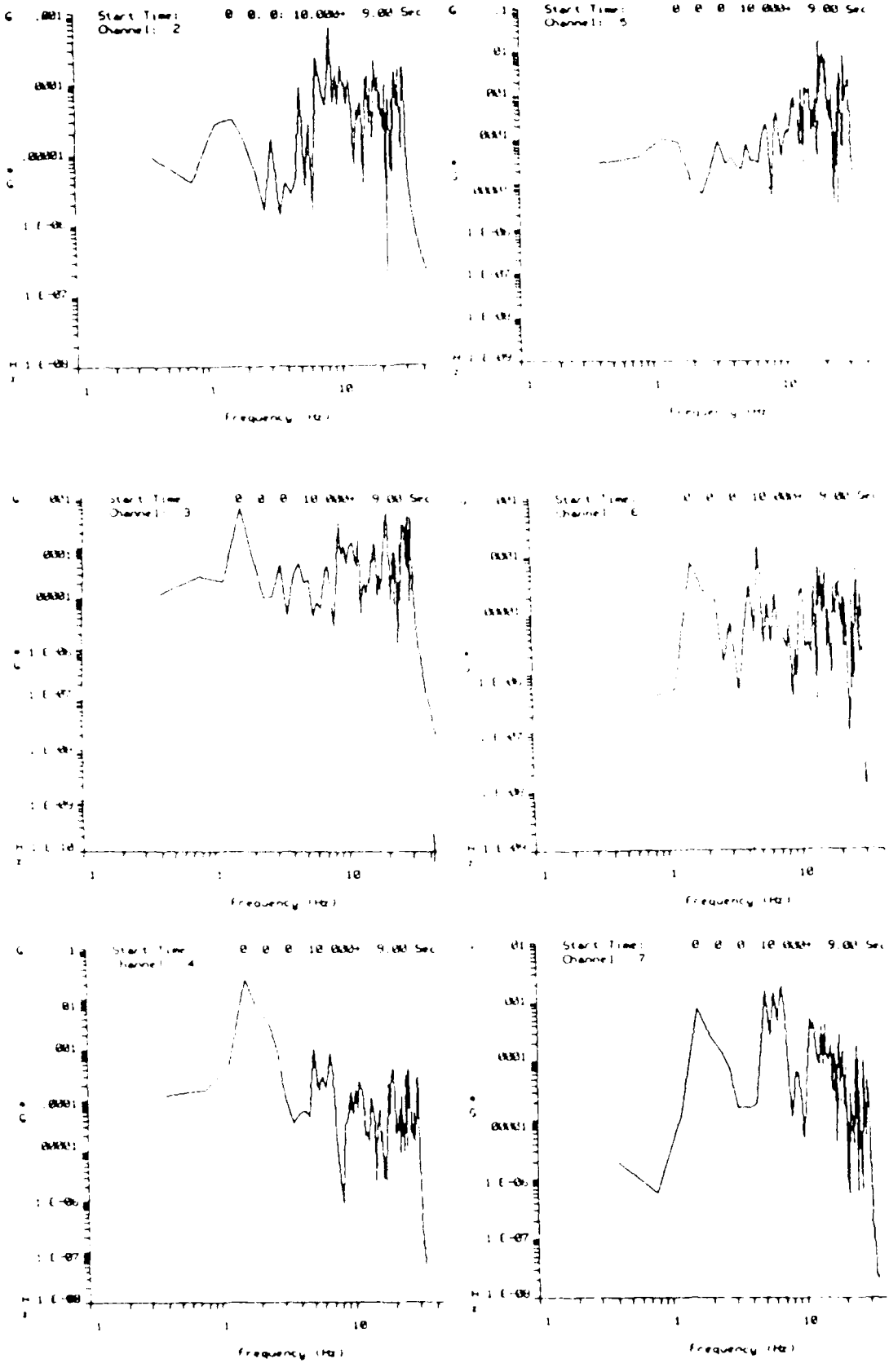

ACCELERATION SPECTRA ESTIMATES: PCR

Figure 14

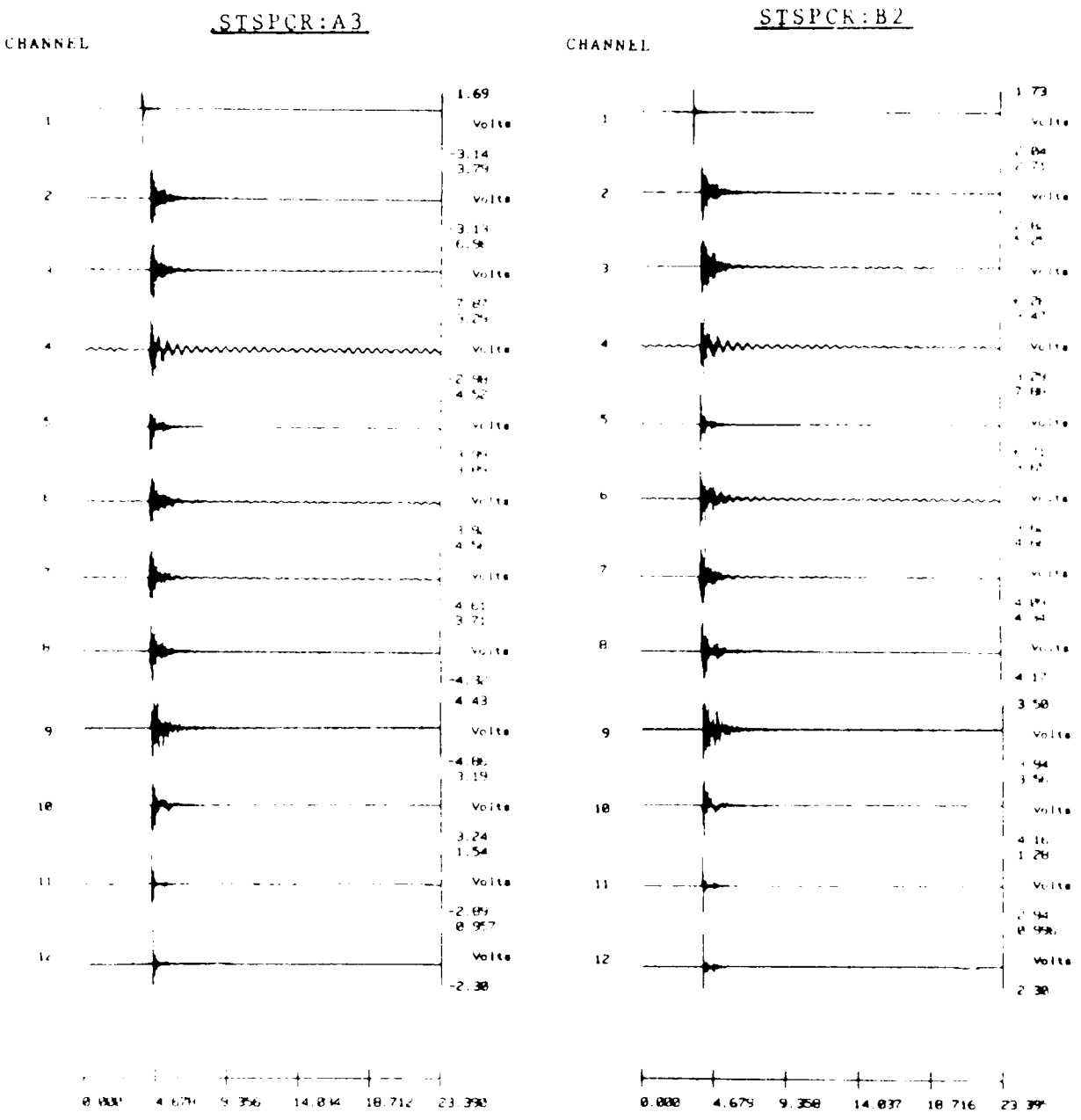


WAVELETS PRODUCED BY A 2.5 POUND SHOT

Figure 3A

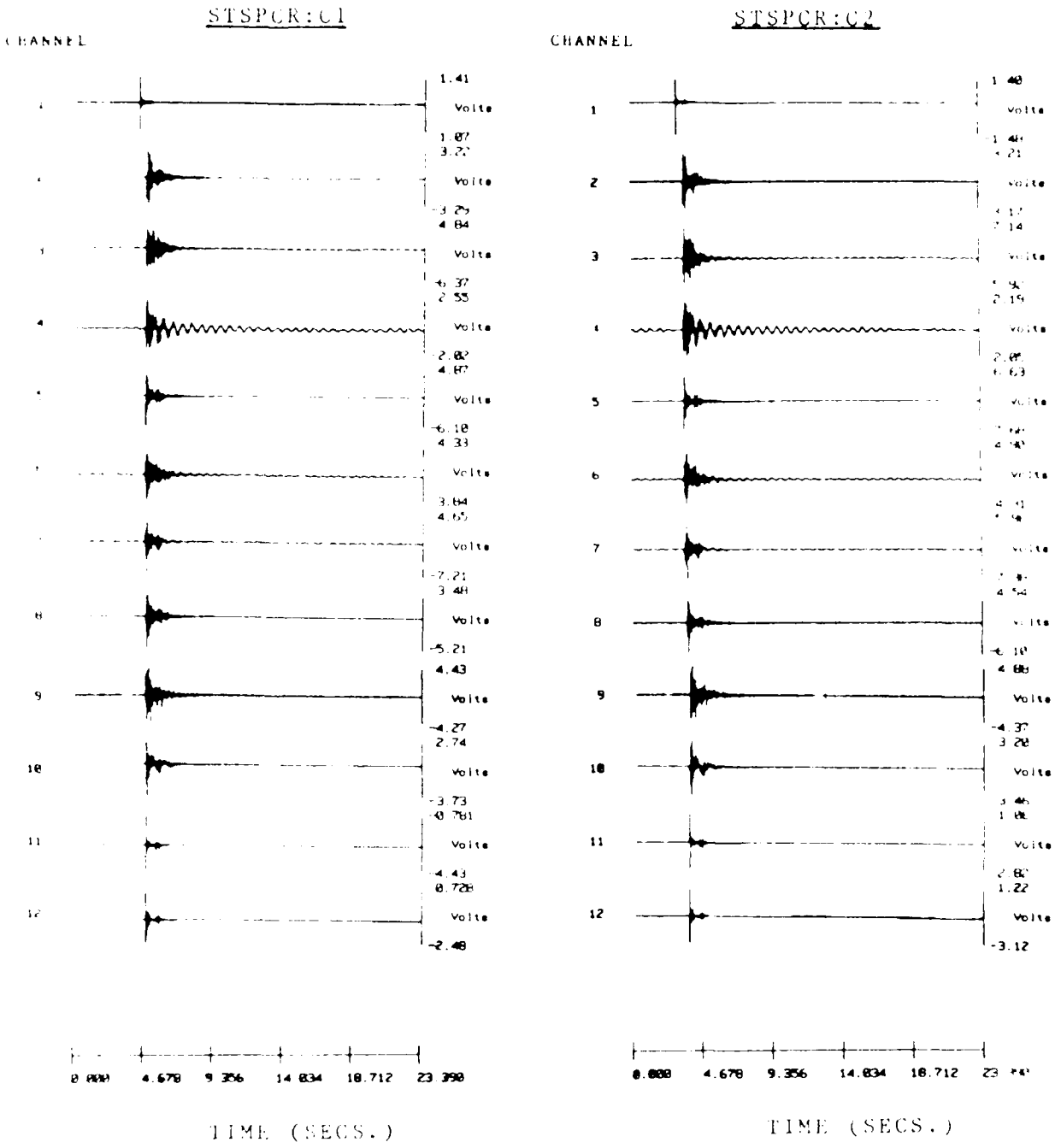


WAVELETS PRODUCED BY A 2.5 POUND SHOT

Figure 4A

## APPENDIX B: FLAT-EARTH VIBRO-ACOUSTICS

Pressure and seismic transients produced by 2.5 and 5.0 pound charges were measured at the EOD Test Range at VAFB. The range is a flat area largely free of surface obstacles. Boundary acoustics over this site are taken to be much the same as those for the flat open area surrounding Pad 39A at KSC.

Surface pressures produced by air shots at the EOD Range and during Shuttle launches are readily extrapolated over our range of interest as spherical, far-field acoustics on a flat-earth boundary. Differences between pressure measurements of the Shuttle at KSC and explosions at the EOD Range for a common offset are taken to be solely a source attribute. Difference pressures under these restrictions can be mapped into one another by temporal convolution.

Figure 1B is the vibro-acoustic disturbance produced by a 2.5 pound charge at the EOD Range measured through GDAS configured as in Figure 2B with channel responses given in Figure 3B through 5B. The pressure transient is found to propagate without a change in form at a median velocity of 345 m/sec, Figure 6B. The specific acoustic impedance at the surface is $1.7*10^{4}$ dyne sec/cm$^{-3}$ (rayl) for all but the air-coupled term. It is worth noting that an air-coupled frequency as high as encountered here (45 Hz) indicates an extremely shallow alluvial cover (15).

Surface pressure wavelets at the EOD Range differ significantly from

those generated by the same weight charge at V23. Differences in wavelet level, form and duration at a common offset are due to boundary generated pressure terms.

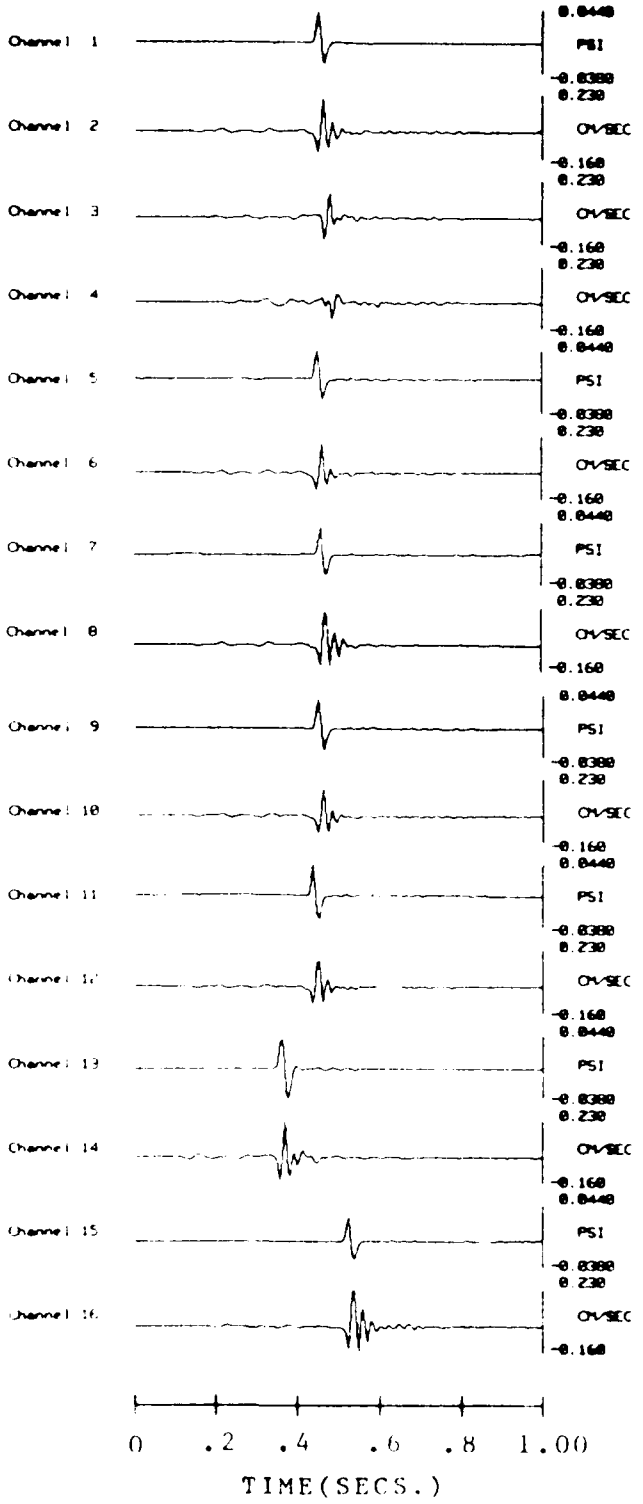


VIBRO-ACOUSTIC SHOT WAVELETS: 1-16

Figure 15

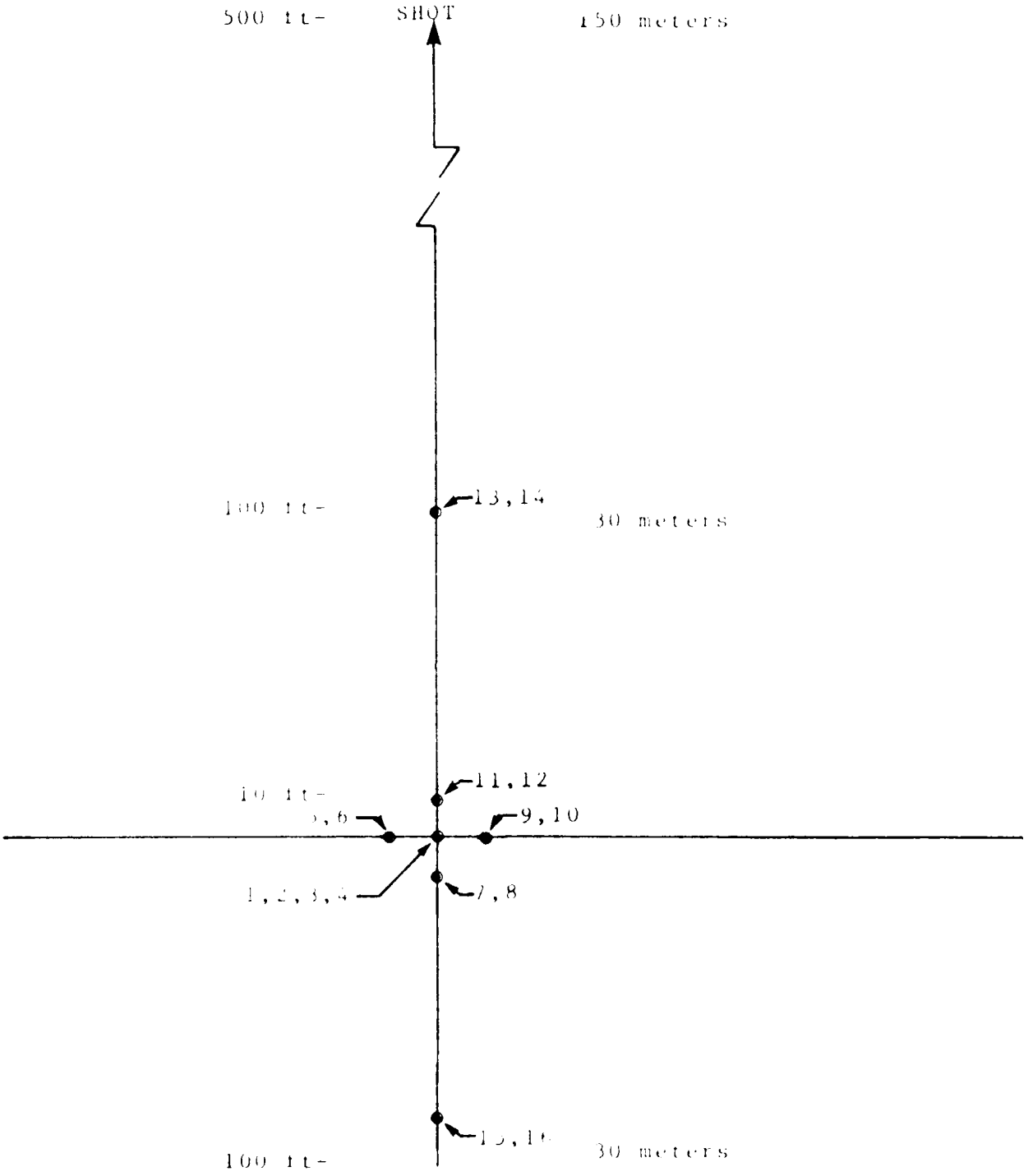


SENSOR CONFIGURATION: VAFB/EOD SHOTS

Figure 2B

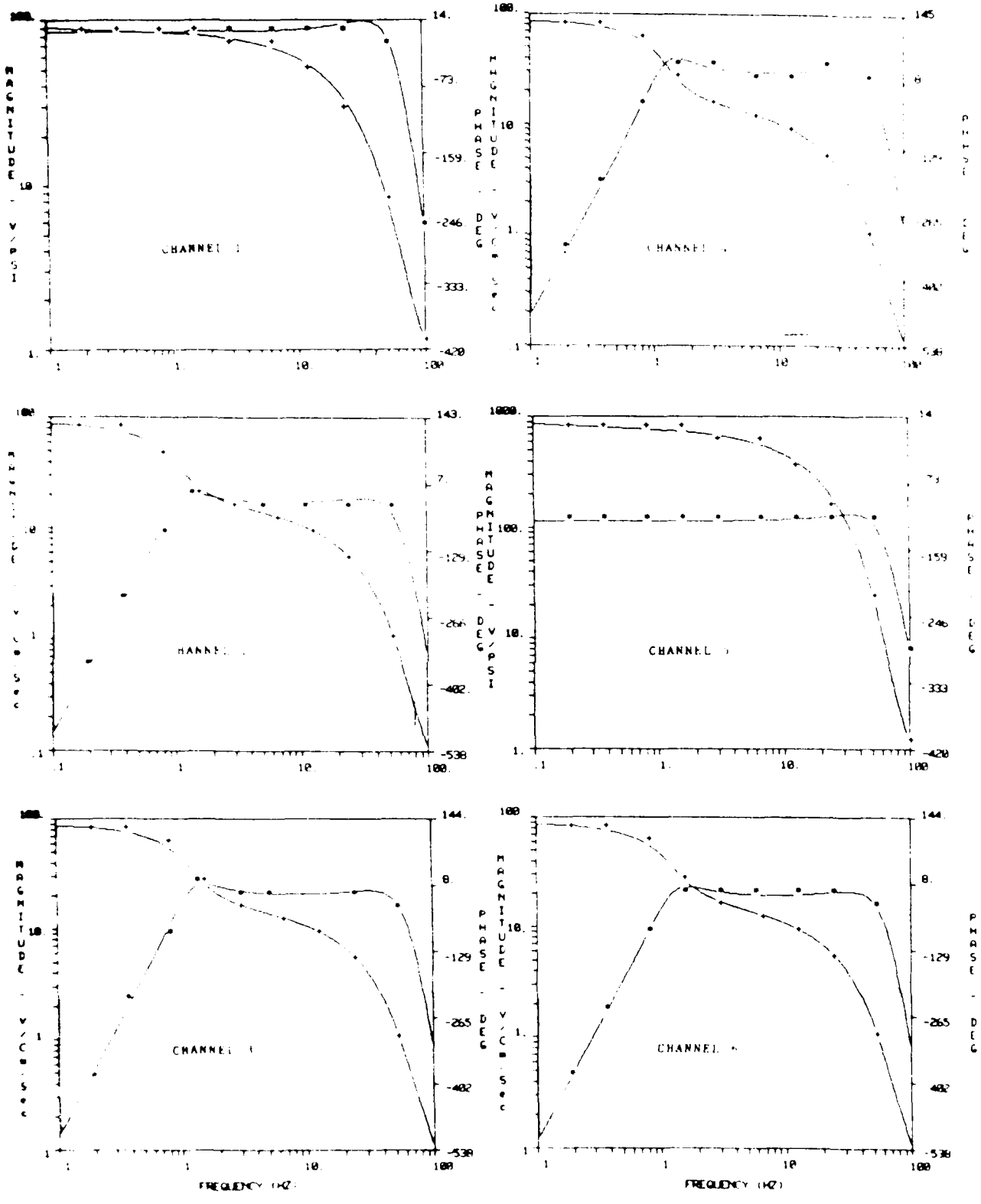


CHANNEL RESPONSES: 1-6

Figure 3B

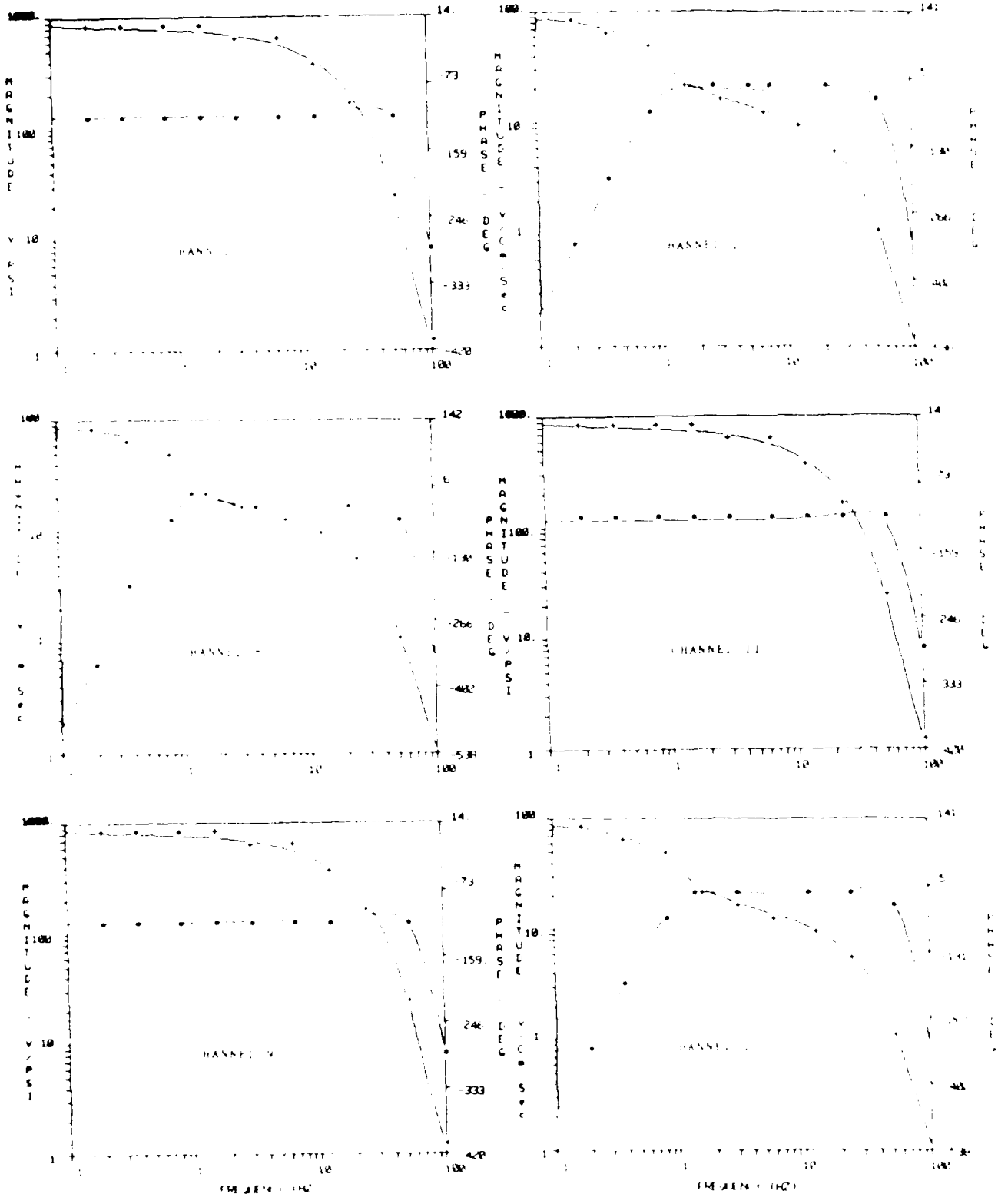

CHANNEL RESPONSES: 7-12

Figure 4b

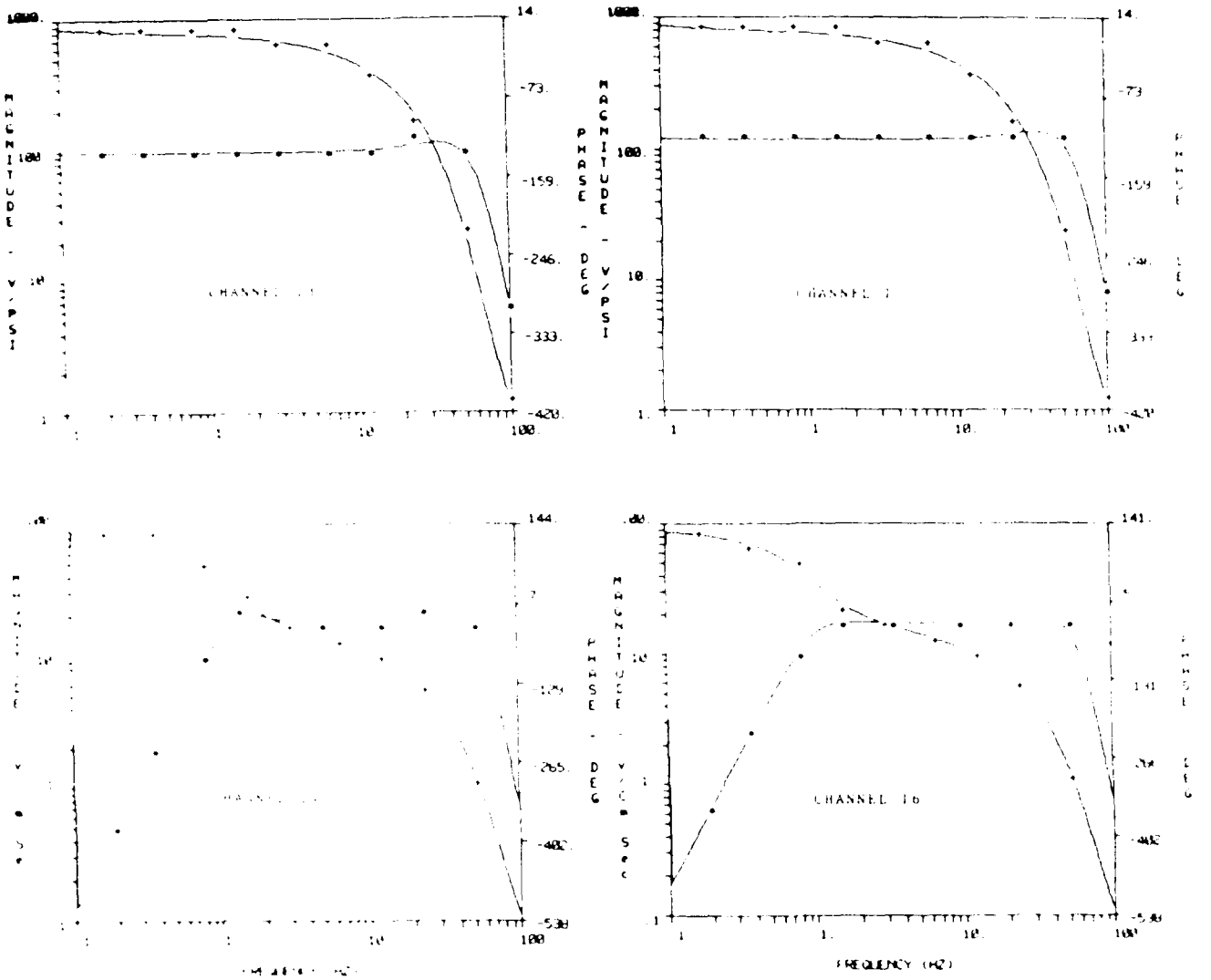


CHANNEL RESPONSES: 13-18

Figure 5B

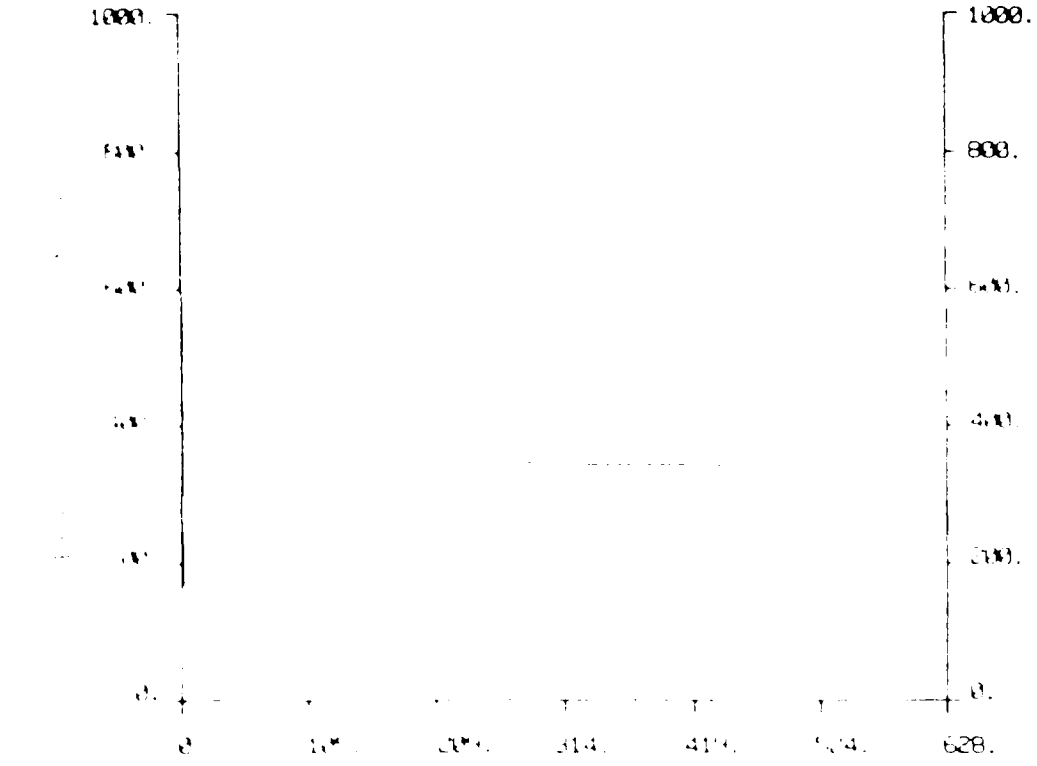


PHASE VELOCITY: VAIB/EOD SHOT WAVELETS

Figure 68

APPENDIX C: PSEUDO VELOCITY SPECTRA

Pseudo velocity spectra are computed from the second order differential equation, $\ddot{y}(t) + a\dot{y}(t) + by(t) = \ddot{x}(t)$, where $\ddot{x}(t)$ is base acceleration and $y$ is the displacement of the structural element, responding as a mechanical oscillator (16). The a's and b's are related to frequency (f) and damping factor (d) as follows: $b = (2\pi f)^2$ and $a = 4\pi df$.

Pseudo velocity spectra call for returning the absolute maximum value of $\dot{y}$, for an ensemble of damping and free period values for the input $\ddot{x}(t)$. Since we have base velocity $v(t)$ available as an output from our simulation we solve for $y$ max by:

$$y(t) + a\int v(t)dt + b\int\int v(\sigma)d\sigma dt = \int v(t)\,dt.$$

The approximating solution (19) for discrete values with $\Delta t = h$ and zero initial condition is given by:

$$y_n = \frac{h\left[\frac{v_n}{2} + \sum_{k=0}^{n-1} v_k - a\sum_{k=0}^{n-1} y_k - bh\sum_{k=0}^{n-1}(n-k)\,y_k\right]}{1 + \frac{ha}{2} + \frac{h^2 B}{4}}$$

The frequencies used range from .25 to 25.0 Hz in increments of .25 Hz.

The y max values are in turn multiplied by the appropriate angular frequencies to give spectra with the units of velocity.

REFERENCES


1. Crowley, F.A., Hartnett, E.B. and Ossing, H.A., Scientific Report No. 3, Amplitude and Phase of Surface Pressure Produced by Space Transportation Systems Mission 5, (Jan 1983), AFGL-TR-83-0039, ADA 125846.

2. Crowley, F.A., Hartnett, E.B., and Fisher, M.A., Scientific Report No. 1, Surface Pressure Produced by Space Transportation System Flight 1E, (Aug 1983), AFGL-TR-84-0213, ADA 150793.

3. Allen, T., Launch Induced Environment Data Book, (Mar 82), Martin Marietta Corp. Report VCR-82-293.

4. Telecon, Ossing, July 1984, Subj: Separation of PCR and AB with PPR at Launch time(confirmed by measurement Aug 1984 and Jan 85.)

5. Wheeler, R.E., Launch Induced Vibration Assessment Study, Part I, Summary Report, (Nov 1982), Martin Marietta Corp. Report VCR-82-337.

6. Brekhovskikh, L.M., Waves in a Layered Media (1960), Acoustics Institute, Academy of Sciences, USSR, Academic Press, Publishers, New York-London.

7. Crowley, F.A., Hartnett, E.B., and Ossing, H.A., Air Force Surveys in Geophysics No. 575, The Seismo-Acoustic Disturbance Produced by a Titan [illegible] with Application to the Space Transportation System Launch

Environment at Vandenberg AFB (Nov 1980), AFGL-TR-80 0358, ADA 100209.

8. Acoustic Loads Generated by the Propulsion System (1971), NASA Report SP-8072.

9. Oppenheim, A.V., and Schafer, R.W., Digital Signal Processing, Prentice-Hall, Inc., Englewood Cliffs, New Jersey.

10. Backus, G., and Mulcahy, M., Moment Tensors and other Phenomenological Descriptions of Seismic Sources - I. Continuous Displacements (1976), Geophys. J.R. Astr. Soc. 46, 341-361.

11. Stump, B., and Johnson, L.R., The determination of Source Properties by the Linear Inversion of Seismograms, (1980), Bull. Seism. Am. Soc. 67, No. 6, 1489-1502.

12. Aki, K. and Richards, P.G. (1980), Quantitative Seismology: Theory and Methods, Vol. I, W.H. Freeman and Co., San Francisco, California, 557 pp.

13. Cessing, R.A., and Crowley, F.A., STS-5 Vibro-Acoustics, (Oct-Nov, 1983), Paper No. 83-2638, AIAA Shuttle Environment and Operations Meeting, Wash, D.C.

14. Von Glahn, P.C., Stand Alone Data Acquisition System: A Function Description, (Oct 1980), Instrumentation Papers No 293, AFGL-TR-80-0317, ADA 100253.

7. Crowley, P.A. and Ossing, E.A., On the Application of Air Coupled Seismic Waves, AFGL-69-0312, (1969), ADA 693132.

8. Bartnett, T.B., A Simulation Study of a Twelve Degree of Freedom System (Mar 1977) AFGL-TR-77-0061, ADA 044756.

9. Iwasaki, F. and Tritunac, M., Characterization of Response Spectra through the Statistics of Oscillator Response, BSSA, Vol. 64, No. 1, pp. 29 - 49, (Feb 1974).

10. Gumbel, E., Statistics of Extremes, Columbia University Press, (1960).

11. A Discrete-time Approach for Systems Analysis, Guenod and Durling, Academic Press, New York and London, 1969.

# ACRONYMS AND ABBREVIATIONS

| | |
|---|---|
| AFGL | Air Force Geophysics Laboratory |
| $a_s$ | Reference Offset |
| AB | Administration Building |
| AT | Access Tower |
| cm | Centimeter |
| d | Threshold Displacement |
| dB | Decibel |
| $E(a_s;t)$ | Empirical Envelope Function at an Offset, $a_s$ |
| EOD | Explosives, Ordinance and Demolition |
| $ESD_{exp}$ | Energy Spectral Density for an Explosion |
| exp | Explosion |
| e | 2.718.82 |
| f | Frequency |
| $f_c$ | Third Octave Band Center Frequency |
| G | Seismic Response |
| GSS | Ground Support System |
| $h_s$ | Source Height |
| k | Wave Number |
| KSC | Kennedy Space Center |
| LCC | Launch Control Center |
| LM | Launch Mount |
| N | Number of Launches |
| $N(0,1)$ | Standard Normal Process (Zero mean, unit variance, white) |

| | |
|---|---|
| OASPL | Overall Sound Power Level |
| OFS | Orbiter Flight Simulator |
| $O(a_s,h;t)$ | Site Pressure Response Term to a Small Source |
| P | Probability |
| $P_{STS}(a_s;t)$ | Launch Generated Surface Overpressure Time History at the Offset $a_s$ |
| $p^{FE}_{STS}(a_s;t)$ | Pressure at a Flat Earth Site Due to Shuttle Source at the Offset $a_s$ |
| $p^{FE}_{exp}(a_s;t)$ | Pressure at a Flat Earth Site Due to an Explosion at the Offset $a_s$ |
| PCR | Payload Changeout Room |
| PGHM | Payload Ground Handling Mechanism |
| PPR | Payload Preparation Room |
| $PSD_{STS}$ | Power Spectral Density for the Shuttle |
| R | Range |
| SATAF | Shuttle Activation Task Force |
| SPB | Support Equipment Building |
| SPL | Sound Power Level |
| STS | Space Transportation System |
| t | Time |
| T | Time Duration |
| $u_i$ | Component Motion |
| VLS | STS Launch Pad Station Set for VAFB |
| VAFB | Vandenberg Air Force Base |
| $\mathcal{L}$ | Mapping Operator |
| $S_{exp}(t)$ | Explosion Source Term |
| $S_{STS}(t)$ | STS Source Term |

| | |
|---|---|
| $\delta(t)$ | Dirac-Delta Function |
| $u_k(x;t)$ | Component Motion at Location x and time t |
| $G_{ki,j...j}$ | The response at a Field Point for a Linear System Excited by a Distributed Source. |
| $M_{i,j...j}$ | Source Description |

END

FILMED

8-85

DTIC